Journal of the Geological Society, London, Vol. **160**, 2003, pp. 57–70. Printed in Great Britain.

Geochemical constraints on the sources of Southern Chile Trench sediments and their recycling in arc magmas of the Southern Andes

ROLF KILIAN[1] & JAN H. BEHRMANN[2]

[1]*Lehrstuhl für Geologie, FB VI, Universität Trier, 54286 Trier, Germany (e-mail: kilian@uni-trier.de)*

[2]*Geologisches Institut, Universität Freiburg, Albertstr. 23 B, 79104 Freiburg, Germany*

Abstract: Pliocene and Pleistocene deep-sea trench sediments cored near the Chile Triple Junction (Ocean Drilling Program Leg 141) were analysed for major and trace element concentrations, and for Sr, Nd and Pb isotopic ratios. Comparisons with the potential source rocks of these sediments suggest little alteration during sediment transport and diagenesis. The sediment compositions reflect exposed area fractions and different erosion rates of upper-crustal rock units of the Southern Andes, indicating that denudation, transport and deposition formed an almost closed system since 2.5 Ma. Pelagic sediments cored farther from the continent (>1000 km) on the Antarctic Plate also contain a significant terrigenous component, mixed variably with hydrogenous precipitates (high Fe–Mn–Th), biogenic barite (high Ba) and opal, but little biogenic carbonate (low CaO and Sr). Our sediment data allow us to estimate the subducted sediment input to southern Andean magmas. Mantle sources of basalts from the Andean southernmost Southern Volcanic Zone (41–47°S) were contaminated by 3–5 vol.% of a terrigenous sediment melt with variable amounts of Ba-rich pelagic sediments, but were not contaminated by slab-derived fluids. Adakites of the Andean Austral Volcanic Zone (49–55°S), formed by melting of a relatively hot subducted slab, contain a variable amount of subducted terrigenous sediment (0–20 vol.% sediment melt) and in some cases Ba-rich pelagic sediments.

Keywords: Southern Andes, Pleistocene, subduction, geochemistry, volcanic arc.

The Southern Chile deep-sea trench (40–50°S; Fig. 1a) is characterized by some of the highest sedimentation rates reported for active continental margins worldwide (0.3–1 m ka^{-1}; Behrmann & Kopf 2001; Lamy *et al*. 2001), probably as a result of the extremely humid and frequently extended glaciations of the continental margin along the Southern Andes (e.g. Clapperton 1990). Balances between tectonically accreted and subducted sediments for the continental margin between 45° and 48°S suggest sediment subduction rates of up to 80 km^3 km^{-1} trench per Ma (Behrmann & Kopf 2001). This is close to the maximum range of sediment subduction rates observed along destructive plate margins worldwide (von Huene & Scholl 1991). Although this continental margin plays an important role in the budget of globally recycled and subducted sediment, little is known about the chemical and isotopic compositions of these deep-sea sediments (see Taylor & Natland 1995; Plank & Langmuir 1998). As Southern Chile Trench sediments are only partly accreted (12% of total sediment; Behrmann & Kopf 2001), they represent equivalents to subducted sediments and allow important constraints on their recycling during subduction-related magmatic processes.

In this paper we present an expanded chemical dataset for Pliocene to Pleistocene Southern Chile Trench sediments, cored by Ocean Drilling Program (OPD) Leg 141 (Fig. 1b–d). We have analysed representative sediments of a fore-arc accretionary wedge at the Southern Andes convergent plate margin (Fig. 1). The chemical and isotopic fingerprints of the Chile Trench sediments and Andean crustal lithologies (Fig. 2) were used to constrain the nature and composition of the sediment flux from the Southern Andes destructive plate margin to the southeastern part of the Pacific Ocean (Figs 1 and 2). By comparing the sediments with potential terrigenous sediment sources, we have also evaluated possible inter-element modifications caused by chemical alteration and/or hydrodynamic fractionation during sediment transport. Chemical compositions of deep-sea sediments cored farther from the South American continent (>1000 km; Fig. 1a) on the Antarctic oceanic plate were also investigated to establish differences in composition that can be attributed to reduced terrigenous and increased biogenic and/or hydrogenous contributions. Furthermore, we use various chemical and isotopic tracers to constrain the element flux from subducted sediments to primary magmas of the Southern Andes (41–55°S; Fig. 1e).

Geology and tectonic setting of the Chile Triple Junction, and OPD Leg 141

The Chile Rise active spreading ridge is being subducted beneath the South American active continental margin at 46°12′S latitude (Figs 1 and 2; Herron *et al*. 1977, 1981). This plate tectonic configuration forms the Chile Triple Junction, which is defined by the Nazca, Antarctic and South American plates. Present-day rates of total sea-floor spreading at the Chile Ridge are 6 cm a^{-1} (Cande & Kent 1992). The Nazca Plate is being subducted beneath South America at a rate of 8–9 cm a^{-1} in a direction slightly north of east, whereas the Antarctic Plate is subducted at a rate of about 2–3 cm a^{-1} in a direction slightly south of east beneath the continental margin (Cande & Leslie 1986). This type of kinematics probably has governed the relative motions of the three plates at least since the late Miocene. The triple point has migrated northward since the Chile Ridge first collided with the South American continental margin near Tierra del Fuego, at about 15 Ma.

Sites 859–861 of ODP Leg 141 were drilled into the fore-arc accretionary prism and its slope cover that are overriding the Nazca Plate just north of the Chile Triple Junction (Fig. 1; Behrmann *et al*. 1992, 1994). Site 863 is located at the toe of the landward trench slope above the subducted Chile Ridge, just

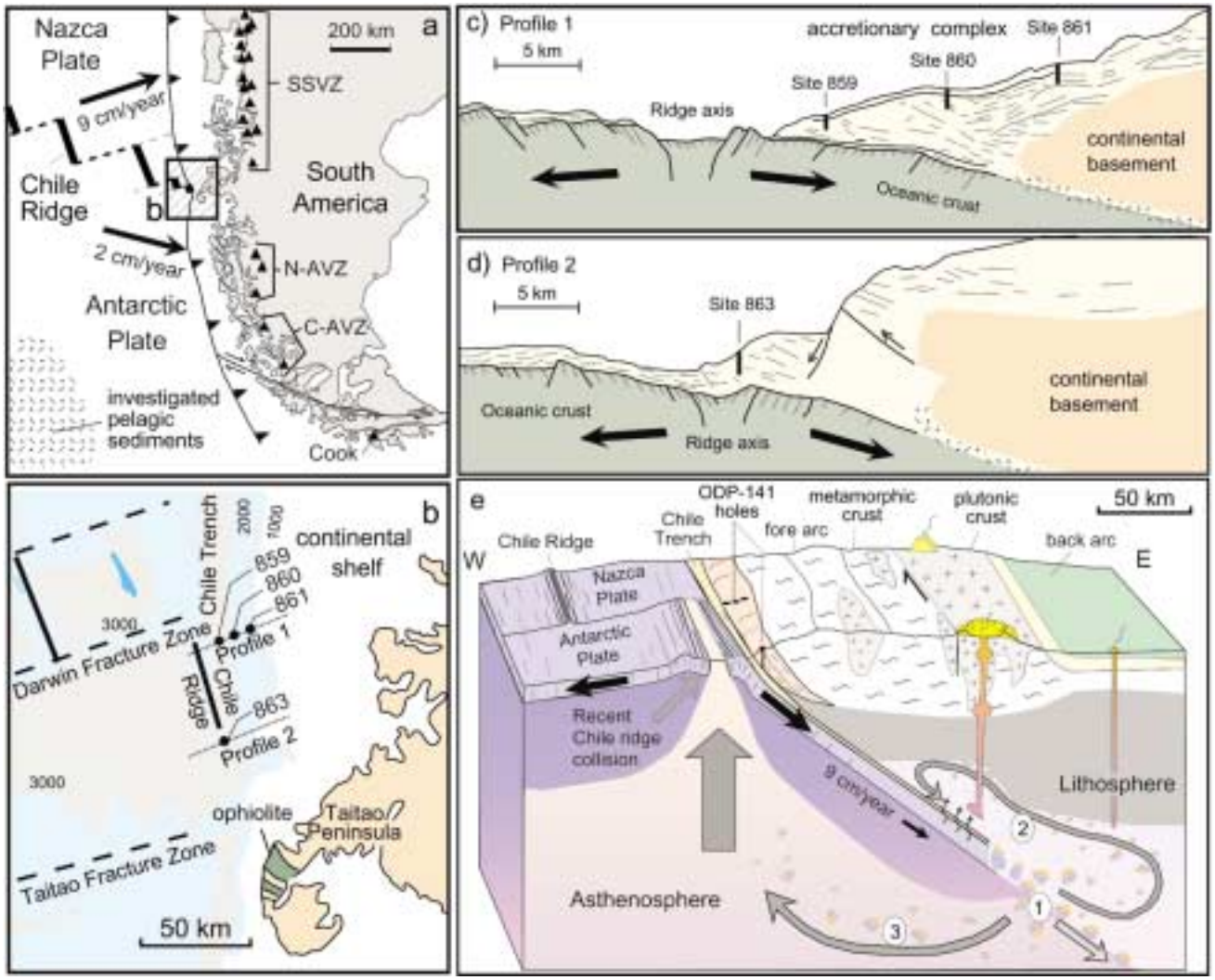

Fig. 1. (**a**) Plate tectonic framework of southern South America and surrounding ocean plates, and the major magmatic provinces: Andean southernmost Southern Volcanic Zone (SSVZ), Andean Austral Volcanic Zone, including a northern part (N-AVZ), a central part (C-AVZ) and Cook volcano. Also shown is the area of the investigated pelagic sediments. (**b**) A local section of the general map shows the positions of the investigated sites (859–861 and 863) of ODP Leg 141 and seismic profiles (Behrmann *et al*. 1994). (**c**) and (**d**) Profiles 1 and 2, illustrating geological and tectonic structures of the Chile Ridge and the accretionary wedge. (**e**) Schematic block diagram showing the collision zone of the Chile Rise with the South American continent and the main crustal units of the continental margin (Palaeozoic metamorphic rocks and Patagonian Batholith). Possible areas of subducted sediment recycling under the Southern Andes comprise: (1) deep mantle regions, where sediments may be recycled in mantle plumes, (2) the asthenospheric mantle wedge; (3) shallow asthenosphere (<200 km depth), where sediments are incorporated in the mantle source of Chile Rise basalts (Klein & Karsten 1995).

south of the Chile Triple Junction. The sediments recovered are of Early Pleistocene to Late Pliocene age (1.5–3 Ma). Seismic profiles of the sediment structures in the Chile Trench environment suggest that large amounts of sediments (up to 80 vol.%), similar in lithology to the accreted and drilled samples, are at present subducted beneath the South American arc and fore-arc (Behrmann & Kopf 2001, Fig. 1e).

Petrography and sampling

The sediments cored at Sites 859–861 and 863 (Fig. 1) are mainly silty claystones, clayey siltstones, siltstones and sandstones. At Sites 860 and 861 there are also intercalated layers of gravel. Tephra layers are not observed, probably because of the predominantly eastward distribution of the arc volcanic fallout (Stern 1991). Detailed descriptions of the sediments and the stratigraphic sequences have been given by Behrmann *et al*. (1992) and Strand (1995). Textural (Diemer & Forsythe 1995) and compositional (Kurnosov *et al*. 1995) variations between the sites are very minor, indicating an absence of marked changes in the sedimentary environment and the source region characteristics in both time and space. The sandstones and siltstones contain quartz, unweathered feldspar, detrital biotite and pyroclastic material as main components, with subordinate hornblende and clinopyroxene. Phyllosilicate mineralogy shows a dominance of illite and chlorite over smectite at Sites 859–861 and the upper part of Site 863. Samples from the lower part of Site 863 (400–720 m) are dominated by smectite. This is probably a diagenetic effect triggered by the migration of thermal fluids through the toe of the accretionary prism (Behrmann *et al*. 1994). We have selected 42 samples of clays, silty and sandy clays, silty and sandy claystones, siltstones and clayey siltstones from Sites 859–861 and 863. Our sampling concentrated on accreted Late Pliocene and Early Pliocene rocks scraped off the downgoing Nazca Plate (Fig. 1). Coarse clastic sediments, such as sands or gravels, were not sampled, to avoid imperfect mixing and mineralogical homogenization on the scale of the 50 cm^3 specimens. However,

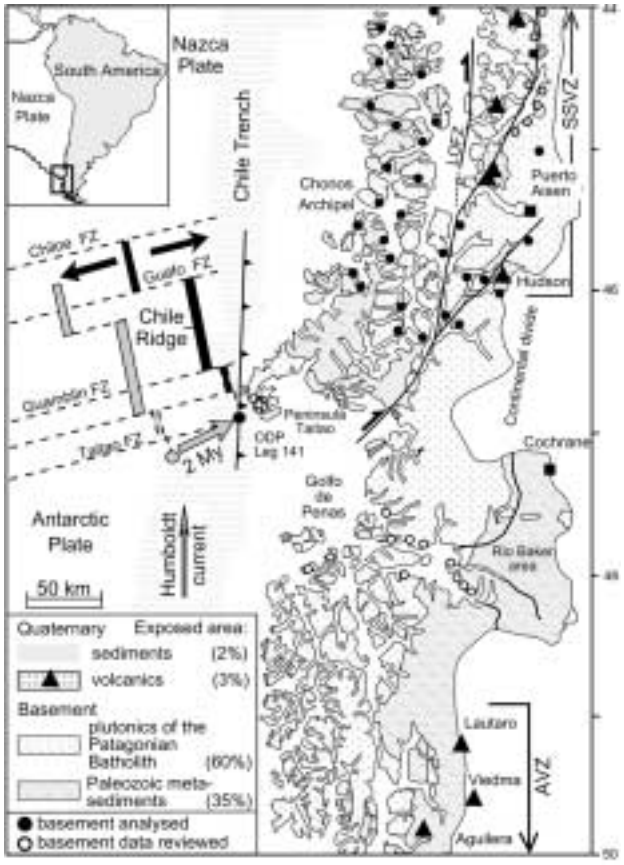

Fig. 2. Geological map of the southern Andean continental margin between 44 and 50°S, showing the dominant lithologies of the crystalline basement and the positions of the Andean southernmost Southern Volcanic Zone (SSVZ) and northern Andean Austral Volcanic Zone (N-AVZ), respectively. The proportions of rock types exposed today are calculated assuming that similar lithologies have contributed to the terrigenous sediment input to the Chile Trench during the Pliocene–Pleistocene. Localities of basement samples investigated and reviewed in this study are indicated. Also shown is the present geometry of the Chile Rise ridge–transform system, and the position of the Chile Ridge (grey) and triple junction between the Antarctic, Nazca and South American plates about 2.5 Ma ago.

coarse clastic deposits represent only a small volume fraction of the sediments cored (Behrmann *et al*. 1992). Care was taken to restrict sampling to core intervals that were not fractured or otherwise disturbed by drilling action.

Analytical techniques

Major and trace elements of sediments and bulk rocks were analysed with a Siemens SRS 300 XRF spectrometer at the Geochemical Institute of Heidelberg University. Major elements were determined on fused discs, whereas trace elements (Cr, Ni, Cu, Sc, V, Zn, Rb, Ba, Sr, Nb, Zr and Y) were measured on pressed powder tablets. All given values are significantly higher than the detection limit of the trace elements (<2–5 ppm). Depending on the composition of the samples, two international standards were chosen and measured within each run of 10 samples for quality control. Deviation from the standards was less than ±2% for the major and ±5% for trace elements. The same trace elements and further trace elements (e.g. Cs, Th, U, Ta and REE) were analysed by inductively coupled plasma mass spectroscopy (ICP-MS), at Newfoundland University, St. Johns, Canada. Methods for sample preparation and acid digestion have been given by Longerich *et al*. (1990). The international standards CCRMP MRG-1 and NIST SRM-688 (BR-688) were measured within each run of 20 samples. Deviation from the standards was less than ±5%. Reagent blanks were measured for quality control. (For precision and detection limits, see also Jenner *et al*. (1990).)

Sr, Nd and Pb isotopic compositions were analysed with the Finnigan MAT 262 thermal ionization mass spectrometer at Tübingen University. Sample preparation and measurement conditions, normalization and correction factors have been given by Bach *et al*. (1994). The La Jolla Nd Standard yielded $^{143}Nd/^{144}Nd$ of 0.511872 ± 6 (2s, $n = 5$), NBS 987 Sr standard yielded $^{87}Sr/^{86}Sr$ of 0.710250 ± 15 (2s, $n = 5$). For isotopic analyses of Pb about 100 mg of sample powder was decomposed in HF–HNO_3. The Pb was separated on Teflon columns with an 80 μl bed of AG50W-X 1–8, 100–200 mesh anion exchange resin, purified with 0.6N HBr and eluted with 6N HCl. The Pb isotopes were measured by using single Re filaments with a phosphoric silica gel. A mass-fractionation correction of $0.12 \pm 0.03\%$ a.m.u.$^{-1}$ was applied to the raw Pb data. The within-run precision was $<0.03\%$ a.m.u.$^{-1}$ and the external precision $<0.03\%$ a.m.u.$^{-1}$ (2s) as determined on NBS 981 ($^{206}Pb/^{204}Pb$ 16.938 ± 0.009; $^{207}Pb/^{204}Pb$ 15.491 ± 0.012; $^{208}Pb/^{204}Pb$ 36.704 ± 0.035; $n = 20$).

Chemical characteristics of the deep-sea sediments and their sources

Chile Trench sediments

The 42 investigated trench sediment samples of ODP Leg 141 have andesitic to dacitic chemical compositions with intermediate alkalinity and relatively high Mg-number ($Mg^{2+}/(Fe^{2+}_{tot} + Mg^{2+})$), especially at high SiO_2 contents (Fig. 3). The relatively high Al_2O_3/SiO_2 ratios (0.23–0.31) are consistent with the observed very low content of siliceous microfossils. There is no relative enrichment of CaO (Fig. 3b) and Ba (Fig. 4a), which might have suggested calcareous biogenic components. Relatively low contents of MnO (0.1 wt.% MnO), FeO, Th and REE, as well as no significant Ce anomaly ($Ce/Ce^* = 1.0$–1.05, where Ce^* is an interpolated value for Ce based upon the concentrations of La and Pr; Elderfield & Greaves 1981), exclude hydrogenous ferromanganese precipitates.

All the trace element patterns of the selected 20 sediment samples (Fig. 4a, Table 1) have pronounced negative Nb and Ta anomalies and are similar to those of calc-alkaline, medium-K volcanic rocks from active continental margins and to bulk continental crust (e.g. Taylor & McLennan 1985; Lopez-Escobar *et al*. 1993). Frequency distributions for concentrations of elements that have generally low mobility in aqueous solutions (Ta, Ti, Y, Hf and Nb) show little variability within the sediment sample suite. For example, 80% of all Y concentrations lie between 25 and 30 ppm and 100% of all Ta values are in the range of 0.5–1 ppm. Concentrations of Sr, Rb, Ba, Nd and Zr show a greater scatter. However, 70% of all Sr values are in the range of 275–325 ppm. The large ion lithophile elements U (1–4 ppm), Cs (2–8 ppm), K ($(10–30) \times 10^3$ ppm) and Pb (10–20 ppm) show the largest variations. The relative standard deviations for most elements of sediments from the investigated ODP holes also confirm their relatively homogeneous composition compared with the ranges of the potential crustal source (Fig. 5; see also Table 3).

Ratios of $^{87}Sr/^{86}Sr$ (0.706–0.712) and $^{143}Nd/^{144}Nd$ (0.5130–0.51265) of representative sediments reflect a mixture of rocks form the Patagonian Batholith (I-type) and Palaeozoic metamorphic rocks (S-type) of the Southern Andes (Figs 2, 6 and 7). The isotopic composition of Pb is characterized by crust-related $^{207}Pb/^{204}Pb$ ratios (*c*. 15.63) and $^{206}Pb/^{204}Pb$ ratios (18.66–18.78), and contrasts with the more mid-ocean ridge basalt

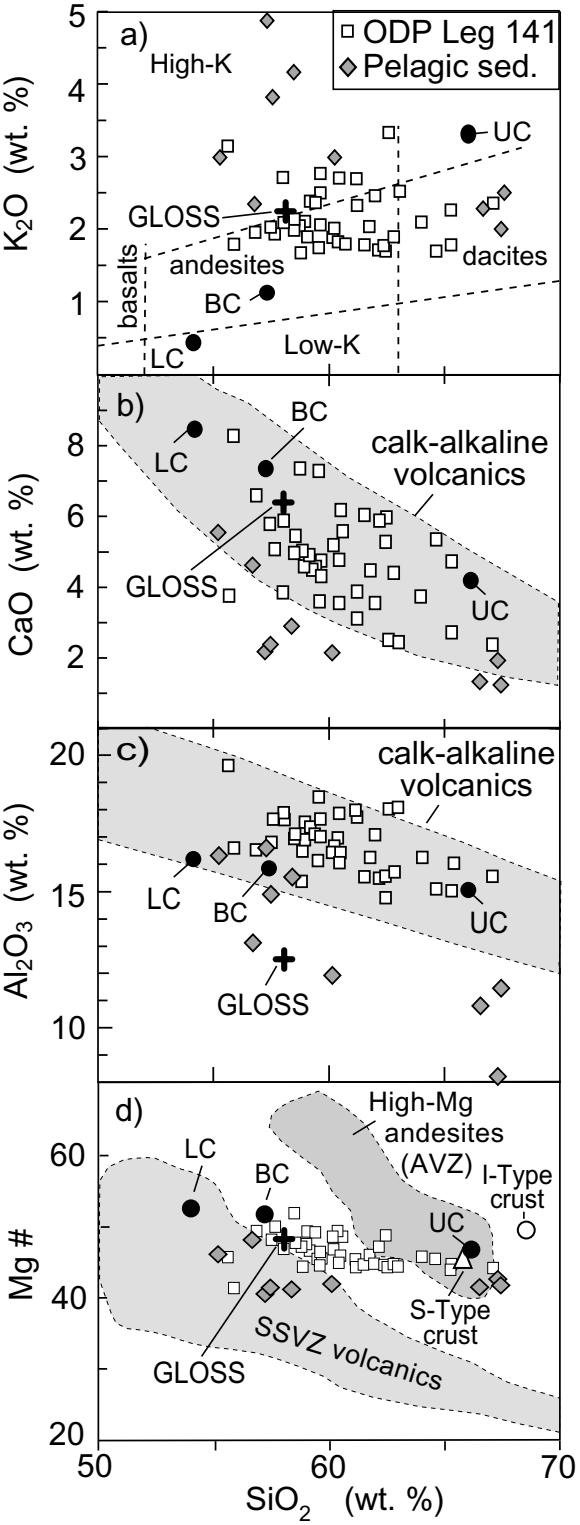

Fig. 3. Contents of (**a**) K_2O, (**b**) CaO, (**c**) Al_2O_3 and (**d**) Mg-number, each plotted v. SiO_2 content for the investigated trench sediments of ODP Leg 141 (□) and pelagic sediments (grey diamonds) from the Antarctic Plate (Fig. 1a). Also shown are average compositions of the upper (UC), lower (LC) and bulk (BC) continental crust (●; Taylor & McLennan 1985), and Global Subducting Sediment (GLOSS; Plank & Langmuir 1998) The chemical variability of medium-K calc-alkaline volcanic rocks of the Andean southernmost Southern Volcanic Zone (SSVZ) and the Andean Austral Volcanic Zone (AVZ) is also illustrated.

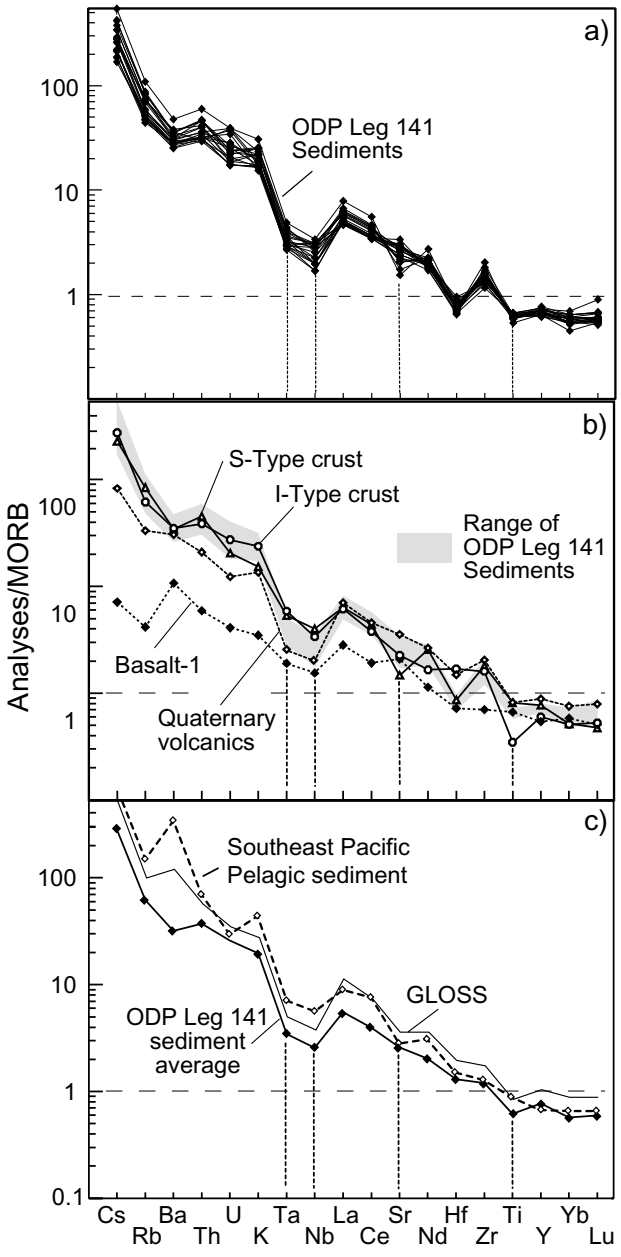

Fig. 4. (**a**) N-MORB-normalized trace element pattern (Sun & McDonough 1989) for the ODP Leg 141 sediments. (**b**) Comparison of the ranges of ODP Leg 141 sediments (grey field) with averages of the Palaeozoic metasedimentary rocks (S-type), plutonic rocks of the Patagonian Batholith (I-type), volcanic rocks from the Quaternary Andean southernmost Southern Volcanic Zone (SSVZ) and Basalt-1 type of the SSVZ (Lopez-Escobar *et al*. 1993; Kilian 1997). (**c**) Comparison of an average ODP Leg 141 sediment with an average of the investigated pelagic sediments from the Antarctic Plate (for location and details, see text and Table 2) and Global Subducting Sediment (GLOSS; Plank & Langmuir 1998).

(MORB)-like pelagic metalliferous sediments from the Pacific ocean floor (Peucker-Ehrenbrink *et al*. 1994).

Sediments deposited far from the continent

Sediments deposited farther from the continent may be also partly accreted and subducted along the Southern Andes. To

Table 1. *Major and trace element content, and Sr, Nd and Pb isotopic data of sediments from holes 859, 860, 861 and 863 of ODP Leg 141*

ODP hole:	859	859	859	859	859	850B	850B	860B	860B	860B	860B	861C	861C	861D	861D	863A	863A	863B	863B	863B
Depth (msfb):	89.2	221.3	287.0	364.3	432.9	119.1	147.1	167.6	281.7	493.7	598.5	172.5	223.8	461.2	477.8	57.3	239.7	355.6	431.4	724.2
Sample no.:	Se-1	Se-3	Se-5	Se-7	Se-9	Se-11	Se-13	Se-15	Se-17	Se-19	Se-22	Se-23	Se-25	Se-27+	Se-29+	Se-32	Se-34	Se-36	Se-39	Se-42
SiO_2	57.17	56.69	58.66	58.98	65.01	60.16	55.18	58.44	58.77	55.98	59.90	56.70	56.56	57.15	59.22	57.34	58.25	58.56	59.28	57.42
TiO_2	0.92	0.96	0.90	0.90	0.78	0.87	0.94	0.93	0.91	0.92	0.84	0.97	0.92	0.85	0.90	0.97	0.89	0.91	0.88	0.95
Al_2O_3	17.74	16.79	16.49	17.36	15.10	15.08	16.15	15.99	17.34	14.67	17.27	16.32	16.21	16.01	17.17	16.83	15.47	15.86	15.06	16.55
$Fe_2O_3{}^{tot}$	7.41	7.31	7.06	7.05	5.69	6.31	7.47	7.07	7.10	7.07	6.37	7.48	7.52	7.49	6.97	7.45	6.76	6.96	6.65	7.19
MnO	0.11	0.11	0.11	0.09	0.07	0.08	0.12	0.12	0.10	0.14	0.10	0.12	0.11	0.09	0.10	0.13	0.10	0.10	0.10	0.11
MgO	2.96	3.51	3.41	2.89	2.23	2.49	3.44	3.08	2.87	3.13	2.49	3.30	3.38	2.95	2.75	3.23	2.82	3.24	2.65	3.45
CaO	3.44	4.71	4.63	2.99	2.29	4.22	5.58	5.06	3.45	7.03	2.33	4.80	4.38	4.88	3.76	4.36	5.95	5.38	5.82	4.47
Na_2O	3.18	3.70	3.61	3.08	3.04	3.59	3.97	3.70	3.27	3.16	2.71	3.78	3.60	3.69	3.08	3.64	3.59	3.36	3.41	3.67
K_2O	2.66	1.82	1.81	2.60	2.29	1.82	1.95	1.83	2.63	1.60	3.19	2.00	2.01	2.01	2.25	2.32	1.74	1.75	1.72	2.31
P_2O_5	0.18	0.25	0.23	0.18	0.17	0.19	0.22	0.22	0.20	0.22	0.17	0.36	0.19	0.18	0.19	0.32	0.23	0.25	0.22	0.28
SO_3	0.16	0.16	0.17	0.28	0.21	0.95	0.96	0.67	0.59	1.35	0.32	0.51	1.05	1.80	0.33	0.33	0.49	0.24	0.56	0.24
H_2O	3.10	2.70	2.30	2.89	3.22	3.47	3.36	2.54	3.34	3.76	3.67	3.06	2.99	2.56	3.12	2.78	3.56	3.18	2.77	3.02
Sum	99.02	98.72	99.37	99.29	100.11	99.23	99.33	99.54	100.58	99.03	99.37	99.39	98.93	99.66	99.83	99.70	99.84	99.79	99.10	99.67
Cr	76	63	57	72	54	57	56	62	62	71	75	58	67	58	63	53	58	54	53	49
Ni	40	42	28	37	21	33	31	63	31	27	29	32	35	38	30	28	35	25	28	28
Cu	31	38	23	40	17	39	37	38	33	29	29	36	52	44	32	31	40	36	31	46
Sc	19	19	21	18	11	21	21	15	21	15	13	19	17	19	16	18	16	17	14	22
V	157	159	151	148	108	143	151	144	154	156	140	151	157	148	153	153	147	140	138	140
Zn	99	97	85	100	77	98	108	104	101	83	133	102	112	91	97	115	113	89	131	103
Rb	105	65	57	99	89	61	67	62	101	53	131	89	71	70	88	85	57	56	61	83
Cs	5.9	3.0	2.6	5.9	4.8	3.1	3.7	3.0	5.3	2.6	7.6	3.6	4.0	3.9	4.8	4.1	3.0	3.1	2.4	3.9
Ba	501	393	393	500	438	387	421	385	493	397	667	506	412	433	465	530	381	352	358	435
Sr	242	339	340	245	206	270	331	317	241	397	182	281	284	308	256	317	359	347	339	303
Pb	15.6	12.8	12.4	15.3	13.4	10.9	13.1	11.2	13.5	11.0	19.6	12.7	14.5	13.9	14.7	14.4	12.3	12.4	10.6	13.0
Th	8.76	6.40	5.91	8.59	8.56	5.85	6.70	5.92	8.57	6.02	11.09	5.60	5.93	6.60	7.45	7.68	5.57	5.47	5.83	7.40
U	1.75	1.39	1.26	1.61	1.92	2.74	2.84	1.85	1.72	2.50	2.86	2.81	2.08	2.01	1.66	1.35	1.50	1.28	1.28	1.45
Ta	0.83	0.63	0.55	0.75	0.80	0.55	0.60	0.57	0.74	0.52	0.92	0.57	0.61	0.56	0.66	0.68	0.55	0.51	0.54	0.68
Nb	9.00	8.00	10.00	11.00	10.00	11.00	7.00	11.00	10.00	7.00	12.00	9	10.00	7.00	11.00	11.00	6.00	6.00	8.00	7.00
Hf	2.43	2.57	2.11	2.06	2.09	1.97	1.92	2.23	2.15	1.87	2.21	2.76	2.30	2.16	2.30	2.02	2.12	2.28	2.22	2.44
Tl	0.53	0.42	0.29	0.55	0.50	0.34	0.35	0.32	0.47	0.29	0.67	0.36	0.39	0.38	0.44	0.48	0.31	0.31	0.27	0.38
Zr	136	133	126	155	203	160	116	163	146	181	170	128	137	155	160	133	141	148	158	140
Y	25	26	24	23	23	22	25	23	24	21	27	25	22	24	23	26	22	25	22	25
La	24.9	22.1	18.0	24.2	26.0	18.6	19.4	18.8	23.6	18.7	30.6	19.6	18.3	20.6	22.9	23.7	19.4	20.0	19.9	22.1
Ce	54.9	48.9	40.9	53.7	55.8	41.4	42.8	41.8	51.8	41.5	66.8	43.7	40.9	46.0	50.5	52.3	41.5	43.8	43.8	49.0
Nd	25.3	23.7	20.3	24.8	24.8	19.2	21.4	20.4	24.0	19.4	30.4	22.0	20.9	22.1	23.7	25.2	20.4	22.1	22.2	24.0
Pr	6.4	5.8	5.0	6.3	6.5	4.9	5.2	5.1	6.2	5.0	7.8	5.4	5.0	5.5	6.0	6.2	5.2	5.5	5.4	6.1
Sm	5.4	5.3	4.6	5.2	5.0	4.3	4.8	4.4	5.3	4.1	6.2	4.9	4.6	4.8	5.0	5.3	4.5	4.9	4.7	5.1
Eu	1.27	1.34	1.18	1.23	1.12	1.01	1.30	1.17	1.14	1.11	1.24	1.23	1.15	1.12	1.18	1.36	1.24	1.28	1.26	1.34
Gd	4.64	5.13	4.26	4.43	4.55	3.82	4.61	4.18	4.53	4.01	5.21	4.94	4.44	4.51	4.61	4.70	4.43	4.57	4.37	4.78
Tb	0.72	0.77	0.68	0.68	0.66	0.57	0.67	0.65	0.66	0.60	0.76	0.70	0.62	0.64	0.69	0.70	0.67	0.65	0.64	0.72
Dy	4.61	4.39	4.01	4.04	3.98	3.65	4.19	3.79	4.05	3.66	4.21	4.30	3.88	3.88	4.07	4.38	4.07	4.27	3.98	4.39
Ho	0.87	0.90	0.87	0.80	0.77	0.72	0.82	0.81	0.80	0.76	0.86	0.93	0.81	0.82	0.80	0.91	0.79	0.81	0.78	0.87
Er	2.57	2.69	2.55	2.38	2.23	2.16	2.40	2.34	2.43	2.20	2.60	2.86	2.35	2.24	2.37	2.52	2.21	2.40	2.30	2.59
Tm	0.37	0.40	0.33	0.31	0.33	0.31	0.37	0.33	0.35	0.30	0.37	0.42	0.36	0.35	0.32	0.36	0.33	0.34	0.33	0.35
Yb	2.30	2.30	2.02	2.09	2.10	1.71	2.43	2.23	1.96	2.07	2.43	2.65	2.22	2.28	2.22	2.15	2.00	2.04	2.10	2.42
Lu	0.33	0.37	0.33	0.34	0.29	0.31	0.38	0.30	0.32	0.31	0.38	0.51	0.34	0.34	0.31	0.35	0.33	0.32	0.33	0.39
$^{87}Sr/^{86}Sr$	0.70817										0.71195		0.70605				0.70614			0.70619
$^{143}Nd/^{144}Nd$	0.51245										0.51232		0.51261				0.51263			0.51264
$^{206}Pb/^{204}Pb$	18.702										18.766						18.653			
$^{207}Pb/^{204}Pb$	15.629										15.640						15.620			
$^{208}Pb/^{204}Pb$	38.705										38.752						38.606			

mbsf, metres below sea floor.

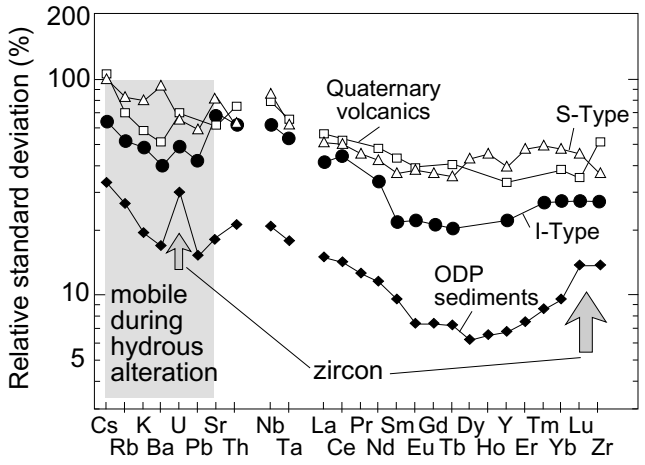

Fig. 5. Relative standard deviation for selected trace elements of sediments from the investigated ODP Sites (859–861 and 863), volcanic rocks of the Quaternary Southern Andes, and plutonic rocks of the Patagonian Batholith (I-type) and Palaeozoic metasedimentary rocks (S-type). Relatively high variations of HREE compared with other REE and of U compared with other LILE may result from only little zircon fractionation or accumulation (indicated by arrows; Grégoire *et al*. 1995).

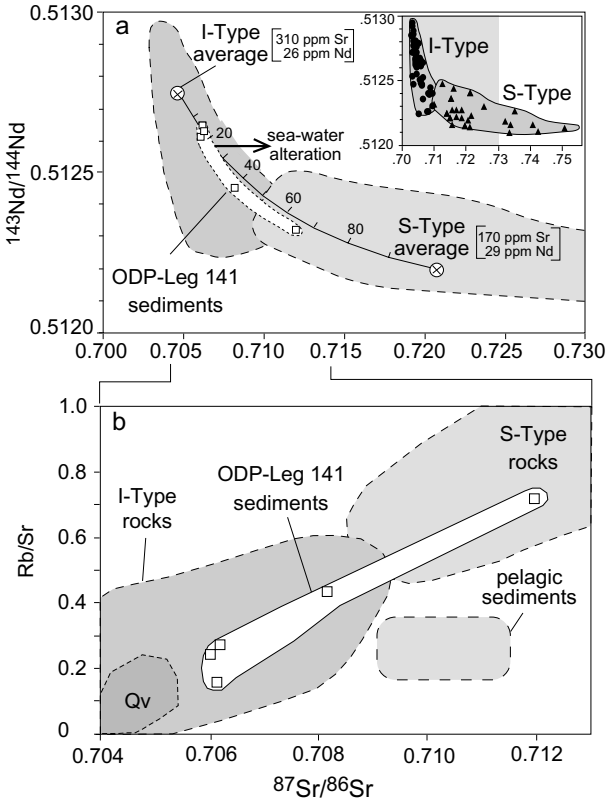

Fig. 6. $^{143}Nd/^{144}Nd$ (**a**) and Rb/Sr ratios (**b**), plotted against $^{87}Sr/^{86}Sr$ ratios for the ODP Leg 141 sediments analysed. Fields show the compositional ranges of Palaeozoic metasedimentary rocks (S-type) and plutonic rocks of the Patagonian Batholith (I-type), and Quaternary volcanic rocks of the Southern Andes (Qv). The inset in (**a**) displays the data defining the I-type and S-type fields. Average compositions for both groups are shown in (**a**) and a mixing line was calculated between these averages. The compositions of ODP Leg 141 sediments plot close to the mixing line, and reflect a contribution of S-type rocks between 10 and 65%. An arrow starting at the mixing line indicates the trend that would result for an average Chile Trench sediment as a result of sea-water alteration (Staudigel *et al*. 1995). Most of the Chile Trench sediments have low Rb/Sr ratios (average of 0.24) suggesting low $^{87}Sr/^{86}Sr$ ratios and a relatively large contribution of Quaternary volcanic rocks and I-type source rocks to the sediment (see also Fig. 7). A range for investigated pelagic sediments from the Antarctic Plate is shown in (**b**).

compare such sediments with the trench sediments, we have investigated Quaternary sediments deposited 1000–1500 km SE of ODP Leg 141 on the Antarctic Plate in water depths of 3953–5531 m (Fig. 1a). These sediments were cored with a piston corer from the German vessel *Polarstern* between latitudes 50°24′S and 69°25′S and longitudes 89°16′W and 97°41′W. The samples are from sediment core depths between 5 and 34 cm. Typical East Pacific sedimentation rates of $(0.2–0.5) \times 10^3$ cm a^{-1} (McMurtry *et al*. 1981) indicate a Late Pleistocene age of 25–170 ka bp. Investigations with a scanning electron microscope show mainly clay minerals (>80 vol.%), some quartz, feldspar and barite, very rare calcite, variable amounts (2–12 vol.%) of siliceous microfossils (mainly diatoms) and 1–3 vol.% manganese micronodules. The major element compositions indicate also a significant proportion of terrigeneous material. The variable, but dominantly high, SiO_2 contents (56–68 wt.%; Fig. 3) and low Al_2O_3/SiO_2 ratios (≤0.12) of these sediments reflect the addition of biogenic opal. The relatively low CaO and Sr (160–450 ppm) contents indicate a limited contribution of biogenic carbonate (Figs 3 and 4c). Higher contents of MnO (0.4 wt.% MnO compared with 0.1 wt.% in the trench sediments), FeO, Th and REE, as well as a positive Ce anomaly (Ce/Ce^* 1.2–1.4), reflect the observed manganese nodules (Elderfield & Greaves 1981; Stoffers *et al*. 1984). The extremely high Ba contents (up to 2500 ppm Ba; Fig. 4, Table 2) are due to barite formation (e.g. Dymond *et al*. 1992). Higher contents of Na_2O (on average 2.2 wt.% higher) and K_2O (Fig. 3) compared with the trench sediments may reflect uptake of Na and K into clay or zeolite minerals (Karl *et al*. 1992).

The Andean crust

For a chemical characterization of the potential Andean source rocks of the Chile Trench sediments we have tried to obtain a chemical dataset of representative crustal rocks with a regional distribution between 43 and 49°S from the area of major Pleistocene denudation as well as representative rocks for the typical crustal lithologies (Fig. 2). The investigated rock types comprise (1) 22 metasediments from the Chonos Archipelago, probably of late Palaeozoic to early Mesozoic age (Miller 1979, 1984), and (2) 12 plutonic rocks of the Patagonian Batholith, representing I-type granitoid crust (Fig. 2; Table 3). Together with the Quaternary volcanic rocks (Lopez-Escobar *et al*. 1993; Stern & Kilian 1996; Kilian 1997), the metasediments and plutonic rocks represent the most likely source rocks of the Chile Trench terrigenous sediments (Figs 1 and 2).

Furthermore, we have incorporated published and unpublished trace element and isotopic data for crustal rocks from the Southern Andes (43–49°S) into our averages (Table 3). Among these are 12 specimens of plutonic rocks from the Taitao Peninsula (H. Martin, unpublished data), plutonic and metamorphic rocks from the Rio Baker area (47–48°S; Weaver *et al*. 1990) and 55 specimens of crystalline basement between 43 and 45°S (Fig. 2), taken from the vicinity of the Liquiñe–Ofqui fault

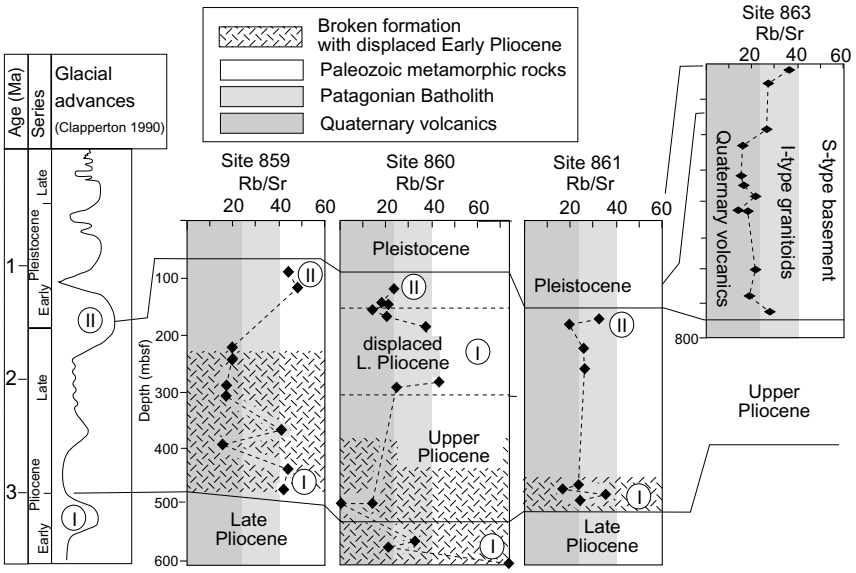

Fig. 7. Rb/Sr ratios of the sediments, plotted v. depth of the ODP holes. Typical Rb/Sr ratios of the main Southern Andes crustal rock lithologies are indicated (Fig. 6). Pliocene to Pleistocene Andean glacial advances (Clapperton 1990) and their approximate stratigraphic relationship to the sediments are illustrated. Major glacial advances (Phases I and II) in the Andes are roughly correlated with high Rb/Sr ratios of the sediments, reflecting a high input of S-type rocks from the Andean fore-arc.

Table 2. *Major and trace element content of pelagic sediments from the Antarctic Plate*

	Sample							
	61	67	75	78	84	86	92	97
SiO_2	56.06	67.43	68.21	68.34	58.12	57.54	59.25	58.34
TiO_2	0.89	0.50	0.43	0.58	0.89	1.65	0.82	0.87
Al_2O_3	16.40	10.96	8.42	12.67	16.68	13.25	15.63	15.00
$Fe_2O_3^{tot}$	7.92	6.42	6.20	5.99	8.41	9.57	8.18	9.43
MnO	0.16	0.75	0.76	0.34	0.17	0.25	0.21	0.38
MgO	3.79	2.89	2.92	2.72	3.20	4.97	3.20	3.73
CaO	5.53	1.29	2.52	1.20	2.14	4.60	2.87	2.35
Na_2O	5.77	6.89	7.90	5.28	4.87	5.20	5.20	5.60
K_2O	3.02	2.31	2.04	2.53	5.10	2.37	4.21	3.86
P_2O_5	0.20	0.09	0.11	0.12	0.20	0.28	0.18	0.16
Sum	99.73	99.55	99.51	99.77	99.76	99.70	99.75	99.72
Li	52	23	24	26	47	52	44	43
Cs	5.54	3.82	3.95	3.58	5.32	4.97	4.57	4.69
Rb	108	66	68	84	169	79	140	128
Ba	1410	3057	3153	1354	990	1372	1075	1326
Sr	320	197	289	162	389	450	411	366
Pb	24.13	21.50	22.04	23.01	22.56	22.89	21.89	23.89
Th	8.65	8.25	7.89	8.42	9.46	8.23	9.25	8.02
U	1.15	1.20	1.25	1.18	1.08	1.11	1.18	1.13
Nb	12.7	14.6	13.8	14.9	12.0	10.2	12.9	10.7
Ta	0.90	1.09	0.95	1.14	1.02	0.86	0.92	0.86
Hf	2.38	3.57	3.21	3.43	2.54	2.27	2.78	2.45
Zr	77	117	162	129	294	240	307	260
Y	22	15	16	15	22	20	20	23
La	23.78	21.00	19.72	20.12	22.24	23.10	24.21	23.08
Ce	54.56	59.52	55.76	56.34	58.12	57.23	61.23	59.23
Pr	6.23	5.65	5.89	6.02	6.12	6.23	5.89	5.78
Nd	24.13	21.50	22.12	23.23	24.02	24.87	23.45	22.98
Sm	5.22	4.83	4.92	5.02	5.23	5.31	5.12	4.98
Eu	1.22	0.96	1.03	0.98	1.09	1.14	1.02	1.21
Gd	4.70	4.11	4.23	4.41	4.78	4.52	4.67	4.81
Tb	0.69	0.60	0.62	0.64	0.68	0.65	0.69	0.70
Dy	4.07	3.71	3.86	3.92	4.04	3.98	4.09	4.11
Ho	0.78	0.67	0.69	0.75	0.81	0.78	0.72	0.76
Er	2.29	1.89	1.92	1.81	2.15	2.05	2.04	2.31
Tm	0.34	0.28	0.31	0.29	0.31	0.29	0.35	0.34
Yb	2.11	1.82	1.93	1.78	2.07	2.01	2.15	2.17
Lu	0.33	0.28	0.27	0.26	0.32	0.31	0.34	0.35

For locations see Figure 1a and text.

Table 3. *Average major and trace element compositions, and compositional ranges for the Andean crustal lithologies, compared with averages of Chile Trench sediments from ODP Leg 141 and pelagic sediments from the Antarctic Plate (Fig. 1)*

	SSVZ volcanic rocks		Andean S-type		PB I-type		Pelagic sediments	ODP 141 sediments	Source mixture
	$n = 87$	Range	$n = 65$	Range	$n = 58$	Range	$n = 8$	$n = 42$	
SiO_2	57.68	50.2–75.5	65.95	43–89	68.62	61–77	61.66	61.20	65.71
TiO_2	1.23	0.1–2.3	1.22	0.2–3.6	0.52	0.1–0.7	0.83	0.95	0.87
Al_2O_3	17.62	1.3–2.1	14.98	9.5–22	15.28	12.0–17.2	13.63	17.10	15.63
FeO^{tot}	7.44	0.5–12.1	6.65	1.3–14	3.61	1.5–6.8	7.77	6.65	5.27
MnO	0.15	0.1–0.2	0.11	0.05–0.4	0.07	0.03–0.12	0.38	0.11	0.10
MgO	3.45	0.2–7.5	3.03	0.6–7.5	1.94	0.1–2.7	3.43	3.21	2.57
CaO	6.91	1.3–10.5	3.52	0.2–10.3	3.29	0.3–4.0	2.81	4.98	4.05
Na_2O	4.05	2.7–6.1	2.89	0.6–5.0	4.10	3.3–4.6	5.84	3.64	3.72
K_2O	1.47	0.4–3.3	1.65	0.1–3.8	2.57	1.5–4.6	3.18	2.16	2.08
Cr	56	<10–262	154	42–340	55	8–78	20	59	85
Ni	31	<10–153	65	15–130	24	<10–38	60	31	37
V	173	<10–337	158	31–412	66	12–113	160	145	114
Pb	10.2	4–22	11.1	2.1–25	16.7	4–21	22.7	13.3	13.7
Zn	81	19–118	84	36–180	50	29–61	115	97	66
Rb	40	11–119	101	4–153	74	64–193	105	74	75
Cs	1.16	0.3–7.8	3.20	0.7–9.6	3.85	1.6–4.6	4.6	3.95	3.12
Ba	427	156–881	482	56–1031	489	276–802	1717	445	474
Sr	421	135–678	173	28–661	267	46–332	323	305	270
Th	3.9	0.7–12.7	8.4	0.3–16.7	7.2	4–13	8.5	6.9	6.9
U	0.9	0.3–2.4	1.5	0.2–2.9	2.0	1.5–3.5	1.2	1.9	1.6
Ta	0.7	0.16–2.2	1.0	0.2–2.0	1.1	0.8–1.4	1.0	0.6	1.0
Nb	6.2	<4–19.9	14.3	4.0–35	9.3	4–14	12.7	9.1	10.1
Hf	4.3	1.9–11.0	2.5	0.6–3.3	4.9	4.0–5.6	2.8	2.2	4.1
Zr	205	76–539	180	46–322	160	131–217	198	149	175
Y	31	11–59	27	12–38	21	10–35	19.1	27	25
La	27.4	8.0–70.1	24.6	6.9–40.3	24.0	12.5–43	22.2	21.5	24.9
Ce	54.9	18.1–108	52.9	16.2–92.1	45.4	25.2–98.1	57.7	47.3	49.6
Pr	8.0	4.2–13.1	6.3	2.1–10.6	4.4	2.2–6.5	6.0	5.7	5.7
Nd	29.7	12.2–56.2	28.6	11.2–38.1	18.6	11.2–35.4	23.3	22.6	23.8
Sm	6.3	2.8–11.6	6.0	1.8–8.7	4.1	2.4–7.5	5.1	4.9	5.1
Eu	1.7	0.5–3.1	1.4	0.5–2.3	0.9	0.7–1.4	1.1	1.2	1.2
Gd	6.7	2.9–10.8	4.8	1.9–7.5	3.5	2.0–3.8	4.6	4.5	4.5
Tb	0.9	0.3–1.5	0.7	0.4–1.1	0.7	0.3–0.8	0.7	0.7	0.7
Dy	6.1	3.5–9.2	4.4	1.8–7.8	3.1	1.9–6.4	4.0	4.1	4.0
Ho	1.45	0.9–2.3	0.84	0.3–1.6	0.85	0.4–1.2	0.75	0.82	0.97
Er	3.48	1.9–5.3	2.38	0.7–4.8	1.67	1.0–3.4	2.1	2.41	2.24
Tm	0.49	0.2–0.8	0.32	0.1–0.7	0.39	0.2–0.5	0.31	0.34	0.39
Yb	2.87	1.5–5.6	1.96	0.6–4.2	1.94	0.8–3.2	2.01	2.18	2.13
Lu	0.45	0.2–0.8	0.27	0.1–0.5	0.30	0.1–0.5	0.31	0.34	0.32
$^{87}Sr/^{86}Sr$	0.70423	0.704–0.705	0.72184	0.71–0.75	0.70613	0.704–0.71		0.70770	0.71040
$^{143}Nd/^{144}Nd$	0.51278	0.5130–0.5126	0.51232	0.5125–0.5121	0.51265	0.5129–0.5123		0.51253	0.51257
$^{206}Pb/^{204}Pb$	18.58	18.5–18.8	18.67		18.67	18.5–18.7			18.65
$^{207}Pb/^{204}Pb$	15.60	15.6–15.7	15.64		15.62	15.5–15.7			15.62
$^{208}Pb/^{204}Pb$	38.50	38.4–38.8	38.78		38.62	38.5–38.7			38.65

PB I-type, plutonic rocks of the Patagonian Batholith; Andean S-type, Palaeozoic plutonic and metasedimentary rocks (for references see text). Major element contents are water-free and normalized to 100%. A best-fit source rock mixture of 50.4% I-type, 29.6% S-type and 20% Quaternary volcanic rocks is given for comparison (for details see text). *n*, number of samples.

zone (LOFZ in Fig. 2; Pankhurst *et al*. 1992; Pankhurst & Hervé 1995; R. J. Pankhurst, unpublished data).

The plutonic rocks of the Patagonian Bathoith are tonalitic, granodioritic, granitic and, in a few cases, gabbroic in composition with mantle-related isotopic signatures (I-type; Table 3). Typical compositional ranges are SiO_2 61–77 wt.%, Al_2O_3 12–17 wt.%, Mg-number 5–55 and K_2O 1.5–4.6 wt.%. Concentrations of incompatible elements (Rb 25–119 ppm, La 12–43 ppm, Th 4–13 ppm) are low to intermediate, taking into account the high degree of fractionation of the plutonic rocks, and the chemical variations shown by standard deviations in Fig. 5 are generally more variable than in the ODP Leg 141 sediments.

With reference to the major and trace element characteristics discussed above, the Palaeozoic metamorphic rocks do not differ significantly from the plutonic rocks of the Patagonian Batholith. However, they have lower Sr contents, a negative Sr anomaly (Fig. 4b) (and thus higher Rb/Sr ratios (Fig. 6b)) and Al_2O_3/CaO ratios of 6–80. Compared with the trench sediments and I-type plutonic rocks of the Patagonian Batholith, they have significantly higher La/Yb ratios (10–30; Fig. 8). Of interest are also the higher $^{87}Sr/^{86}Sr$ ratios and lower $^{143}Nd/^{144}Nd$ ratios of the Palaeozoic metamorphic rocks compared with the I-type plutonic rocks of the Patagonian Batholith (Fig. 6).

In summary, the igneous and metamorphic rocks of the Southern Andes continental margin can be subdivided into three types,

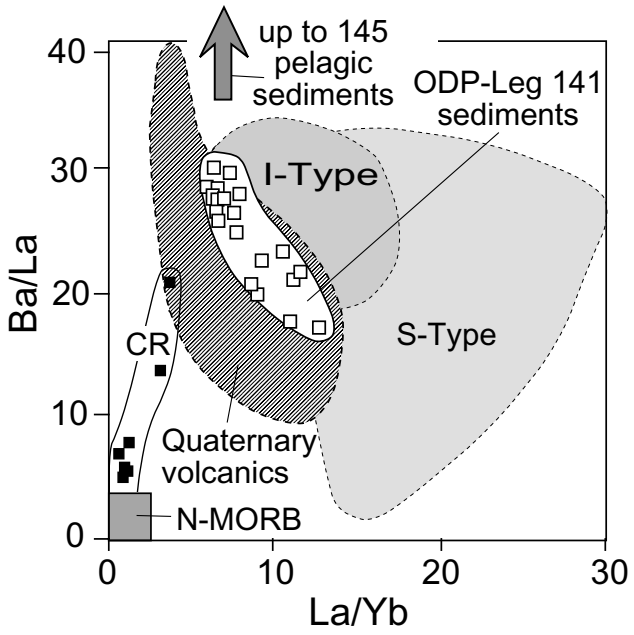

Fig. 8. Ba/La v. La/Yb showing the intermediate composition of the ODP Leg 141 sediments between their major Andean crustal source lithologies (Table 3): Quaternary volcanic rocks, Palaeozoic metasedimentary rocks (S-type) and plutonic rocks of the Patagonian Batholith (I-type). An arrow indicates the extraordinary high Ba/La of the investigated pelagic sediments (Table 2). A trend from N-MORB to the ODP Leg 141 sediments is displayed by Chile Rise basalts (CR: Klein & Karsten 1995).

on geological and geochemical grounds (Figs 2 and 4–8): (1) metasedimentary and metagranitoid Palaeozoic continental basement (S-type) characterized by high Rb/Sr ratios (>0.6) and high $^{87}Sr/^{86}Sr$ ratios; (2) Jurassic to Cenozoic plutonic rocks of the Patagonian Batholith with relatively low Rb/Sr ratios (<0.6) and low $^{87}Sr/^{86}Sr$ ratios (<0.71); (3) Quaternary volcanic rocks of the Southern Andes with basaltic to rhyolitic compositions and generally mantle-related Sr and Nd isotopic signatures. Averages and ranges of the chemical and isotopic data of these crustal lithologies are given in Table 3.

Chemical mass balances on the contributions of typical crustal lithologies in Chile Trench sediments

It is evident from the trace element plots of Figs 4 and 8 that the Chile Trench sediments analysed have a compositional signature intermediate between the three principal lithologies found at the present level of erosion in the Southern Andes (Fig. 2). As discussed above, these sediments were not chemically altered significantly during sediment transport or diagenesis. From this observation, we derive the following two questions: (1) What are the proportions of the sediment-providing crustal lithologies? (2) Are these proportions comparable with the areas of these lithologies exposed today? To provide answers we have used trace element concentrations and Sr and Nd isotope data to calculate mass balances between the compositions of the sediments and its possible sources.

The Sr and Nd isotopic compositions of the Chile Trench sediments reflect the contribution of two types of isotopically contrasting rock types (metamorphic Palaeozoic basement and Jurassic to recent igneous arc rocks) of the Andean continental crust. The inset in Fig. 6a clearly shows the differences in the isotopic signatures. Averages of the two rock types are taken to be the end-members of a mixing line that shows a 15–65 wt.% contribution of Palaeozoic metamorphic rocks in the trench sediments. Most Rb/Sr values of the Chile Trench sediments plot closer to the Andean igneous arc rock end-member of the mixing line, indicating on average only 30% contribution of 'old' Palaeozoic S-type crust to the Chile Trench sediments.

Average trace element contents of the plutonic rocks from the Patagonian Batholith, Palaeozoic metamorphic rocks, Quaternary volcanic rocks and primitive basalts found in the Andean southernmost Southern Volcanic Zone are given in Fig. 4b (and Table 3). It is evident from this diagram that the average Ta, Nb and Ti contents of the sediments are significantly lower than those of the plutonic and metamorphic rocks. A contribution of 20% low-Ta(Nb) Quaternary volcanic rocks of the Southern Andes, in addition to the isotopically constrained 30% S-type crust and 50% I-type crust, is necessary to restrict the Nb and Ta contents to values similar to those of the trench sediments. In the former mixing calculation the negative Sr anomaly of the S-type rocks limits their contribution also to around 30 wt.%. As a result of the former consideration we suggest a best-fit mixture of potential source rocks to reproduce the average sediment composition, comprising 50 wt.% of I-type plutonic rocks, 30 wt.% of S-type rocks and 20 wt.% of Quaternary volcanic rocks (Fig. 9; Table 2). This may be compared with the following area percentages of the same rock types exposed on land today between the Pacific shoreline and the continental divide between 44 and 50°S (Fig. 2): 60% I-type plutonic rocks, 35% S-type rocks and 5% Quaternary volcanic rocks. Both datasets fit reasonably well. However, the calculated proportion of the Quaternary volcanic rocks in the Chile Trench terrigenous sediments (*c*. 20 wt.%) is significantly higher when compared with the recently exposed area of this rock type (<3% of exposed area: Fig. 2). This probably reflects the high erosion rates of the young volcanic rocks and pyroclastic deposits during the Plio-Quaternary glaciation in the Southern Andes. Rapid denudation may also occur because most of the volcanic edifices are on high ground (up to 3200 m altitude) and most pyroclastic deposits are amenable to physical weathering.

Discussion

Chemical modifications during sediment transport and diagenesis

During late Pliocene and early Pleistocene times, most of the eroded crustal material of the Andes between 43 and 49°S reached the Pacific Ocean directly by glaciers or through a fjord system without extensive fluvial transport or redeposition. Therefore, many minerals eroded from the Andean upper crust, especially quartz, pyroxene, amphibole and some heavy minerals, have survived the transport to the deep-sea trench without significant mineralogical or chemical alteration (Kurnosov *et al*. 1995). However, feldspar is mostly altered to illite or smectite in the trench sediments (Behrmann *et al*. 1994). Thus during clay mineral formation some elements (K, Na, Sr and Ba), which are mobile in aqueous solutions, could have been leached or concentrated in the sediments. However, the similar trace element pattern of the Andean crustal source rock lithologies and the trench sediments does not indicate such a process (Fig. 4b). A fractionation or addition of certain elements by transport or diagenesis would result in high standard deviations of elements in the sediment sample suite compared with their potential source rock suites. Figure 5 shows that all trace elements of the

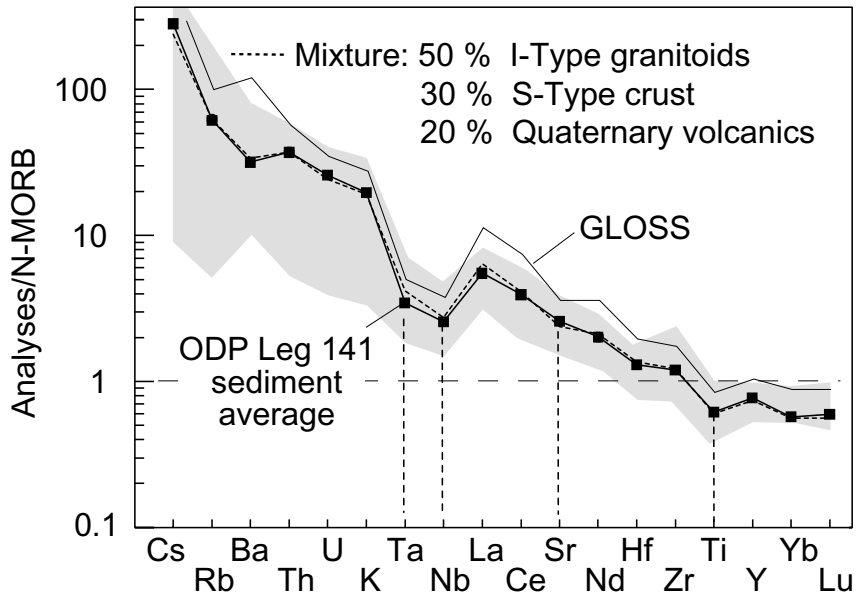

Fig. 9. N-MORB-normalized trace element plots (Sun & McDonough 1989) for an average composition of the trench sediments (continuous line) and a best-fit mixture of 50.4% I-type, 29.6% S-type and 20.0% Quaternary volcanic rocks (dotted line; for details see text). The range of rocks from the continental crust of the Southern Andes is shown as a grey field (Fig. 4 and Table 3).

sediment suite show significantly less chemical variation than the source rocks, suggesting homogenization and no specific element alteration in aqueous or hydrothermal systems. The elements Nb and Ta with a similar chemical behaviour to Ti are commonly little affected during sediment transport and/or hydrogenous alteration (Plank & Langmuir 1998). Therefore, these elements can be used to monitor possible fractionation processes of elements with higher mobility, such as K, Ba, U, Pb and Sr. Figure 5 shows that these mobile elements, with the exception of U, have similar variations to Nb, Ta and Ti. This suggests that the trace element budget was not altered significantly during the sediment transport or diagenesis. Compared with the standard deviations of Nb, Ta and the light rare earth elements (LREE) in the sediment, those of U and the heavy rare earth elements (HREE) are significantly higher (Fig. 5). As the latter elements are highly concentrated in zircon (Grégoire *et al*. 1995), their higher standard deviations and the relatively high Zr/Hf ratios can be explained by variable but minor enrichment (<1 vol.%) of the heavy mineral zircon, a frequent mineral in acid plutonic and metamorphic rocks of the Andes, and very resistant in long-term sedimentary processes. However, such a fractionation would not produce significant changes for other major and trace element concentrations of the trench sediments.

Interstitial fluid chemistry and illite/smectite ratios of the ODP Leg 141 sediment cores suggest that hydrothermal circulation and episodic fluid expulsion have affected the lowermost part of the accretionary wedge (Brown *et al*. 1995). However, our downhole profiles of trace element concentration in the sediments do not indicate a systematic enrichment or depletion in deeper parts of the ODP holes, where hydrothermal effects are estimated to be higher, in particular in the lower section (400–720 m) of Site 863 (Fig. 7). This indicates that the incompatible element budget of the sediments is closed with respect to the interstitial water system. In addition, the Sr and Nd isotopic data of the more I-type related sediments are similar to those for the potential source rocks and do not show a shift towards higher $^{87}Sr/^{86}Sr$ ratios of modern sea water (0.709) at constant $^{143}Nd/^{144}Nd$ ratios (Fig. 6; e.g. Staudigel *et al*. 1995). This suggests no significant exchange of Sr between sediments and sea-water-derived pore fluids. Furthermore, relatively high $^{207}Pb/^{204}Pb$ ratios (15.63–15.64) of the Chile Trench sediments are typical for the upper continental crust of the Southern Andes and are in contrast to metalliferous Pacific sediments, which reflect hydrothermal Pb exchange with altered MORB (Peucker-Ehrenbrink *et al*. 1994).

Sediment sources

The chemical composition of the Chile Trench sediments was modelled by a variable contribution from the major crustal lithologies of the Southern Andes. This high terrigenous input is probably due to the high sedimentation rates ($\leqslant$1 mm a^{-1}) in the Southern Chile Trench (Lamy *et al*. 2001). The chemical characteristics also exclude significant contributions of biogenic calcite, barite and/or opal as well as ferromanganese nodules.

The stratigraphical relations of downhole Rb/Sr ratios of the Chile Trench sediments (Fig. 7) show irregular variations in the Rb/Sr ratios and two sedimentation phases with relatively high Rb/Sr ratios. Among the three main sediment source rocks from the Andean crust described above, only Palaeozoic metamorphic rocks are characterized by high Rb/Sr ratios (Fig. 6b). This suggests two sedimentation phases with a high contribution of S-type rocks to the Chile Trench sediments (Fig. 7), one phase in the mid-Pliocene (3–3.5 Ma) and another phase in Late Pliocene–Early Pleistocene (2–1.5 Ma). These phases correspond reasonably well to periods of major glacial advances up to the Andean fore-arc (Clapperton 1990). These glacial advances could have increased erosion of the Palaeozoic rocks exposed mainly in the Andean fore-arc (Fig. 2).

The investigated pelagic sediments, which were deposited far from the continent, represent lower sedimentation rates (0.2–0.5 cm ka^{-1}; McMurtry *et al*. 1981). Petrographical characteristics and relatively high Ti, Nb and Ta contents of these sediments also indicate a significant terrigenous component (>80 vol.%), but they are chemically modified by variable contributions of biogenic opal (2–12 vol.%) and manganese micronodules (1–3 vol.%). The latter lead to higher MnO, FeO, Th and REE, and lower U/Th ratios as well as a positive Ce anomaly (Ce/Ce^* 1.2–1.4; Elderfield & Greaves 1981; Stoffers *et al*. 1984), if compared with the trench sediments. Some formation of barite in the pelagic sediments is reflected by high Ba contents (up to 2500 ppm Ba; Fig. 4, Table 2), and high Ba/La (up to 145) and Ba/Th ratios (positive Ba peak; Fig. 4b), if compared with the Chile Trench sediments and the Andean crust.

As a result of Na and K uptake into clay or zeolite minerals (Karl *et al*. 1992), the investigated pelagic sediments have higher Na_2O and K_2O contents (Fig. 3), and K/U ratios than the trench sediments. None of the investigated pelagic sediments contain detectable proportions of calcareous nannofossils, which elsewhere are a significant component of western Pacific pelagic clay. In contrast to our samples, such pelagic deposits have very high Sr and Ba contents, low REE contents, low Ba/Sr ratios and negative Ce anomalies (Hole *et al*. 1984). The overall trace element contents of the Chile Trench sediments are lower, but the shapes of the trace element patterns are similar to those of the average Global Subducted Sediment (GLOSS: Plank & Langmuir 1998), except for lower relative Ba contents (Fig. 4b).

Sediment recycling into the mantle and arc magmas

Geological, tectonic and climatic conditions along the southern Andean continental margin between 42 and 52°S (Fig. 1a; Cande & Leslie 1986), as well as mass balances between eroded Andean crust and accreted sediments, suggest that a significant amount of sediment (*c*. 80% of the total sediment input and up to 80 km^3 sediment subduction km^{-1} trench per Ma; Behrmann & Kopf 2001) was subducted below the Andean arc during the Pliocene and Pleistocene. Sediments that are subducted near the plate triple junction, where the oceanic crust is only few million years old, are likely to be chemically similar to the investigated sediments of ODP Leg 141. Further to the south or the north, where the subducted plate becomes older (>20 Ma), a higher pelagic sediment component could have been subducted. Using trace element and isotopic signatures, we now discuss the possible contribution of the various investigated sediment types to primary Andean magmas.

Chemical and isotopic signatures of subducted sediments are often detected in rocks of volcanic arcs (e.g. Hawkesworth & Ellam 1989; Hawkesworth *et al*. 1991, 1997; Plank & Langmuir 1993; Pearce *et al*. 1994; Elliott *et al*. 1997). The 'subduction component' of primary Andean arc magmas may have originated from more or less altered basalts of the subducted oceanic plates and from overlying sediments. Depending on the thermal structure of the slab subducted below the Southern Andes, either fluids or partial melts or both are formed in the subducted slab and contaminate the overlying mantle wedge (e.g. Peacock *et al*. 1994; Stern & Kilian 1996; Kilian 1997; Kilian & Stern 2002). These different processes produce different element transfer and enrichment in primary arc magmas. The elements Ba, Pb, Rb, K, U and Sr are highly distributed into fluids generated either in subducted MORB or subducted sediments (Brenan *et al*. 1995; Elliott *et al*. 1997; Hawkesworth *et al*. 1997). Experimental results suggest that Th, Nb, Ta, Ti and REE are not dissolved in such hydrous fluids (Keppler 1996; Ayers *et al*. 1997). In the subducted slab rutile generally retains high field strength elements (e.g. Ti, Nb and Ta; Brenan *et al*. 1994), whereas in asthenospheric sources or the mantle wedge these elements are commonly partitioned into partial melts (e.g. LaTourrette & Burnett 1992; Niu & Hékinian 1997). Th and LREE are also thought to be predominantly partitioned into partial melts of the subducted slab (e.g. LaTourrette *et al*. 1993; Schiano *et al*. 1995; Stern & Kilian 1996). These observations suggest that high Ba/Th, Ba/La, Pb/Ce and U/Th ratios characterize fluid-dominated subduction components, whereas high Th/Nb and La/Nb ratios characterize slab-melt contributions (Elliott *et al*. 1997; Hawkesworth *et al*. 1997). Furthermore, relatively high $^{87}Sr/^{86}Sr$ and $^{207}Pb/^{204}Pb$ ratios of arc magmas can be produced by slab fluids or slab melts, whereas low $^{143}Nd/^{144}Nd$ ratios can reflect contamination by bulk subducted sediment or melts derived therefrom, but not by slab fluids.

Sediment recycling in Chile Ridge basalts

Fresh basaltic glasses of the Chile spreading ridge reflect the composition of MORB subducted below the Southern Andes (Figs 1 and 2; Klein & Karsten 1995) as well as trace element and isotopic signatures of the regional asthenosphere. Most of these basalts have N-MORB-like chemical and isotopic characteristics (Sun & McDonough 1989; Figs 8, 10 and 11): low Ba/La (<5), Ba/Th <50, U/Nb <0.05, $^{87}Sr/^{86}Sr$ in the range 0.7023–0.7028 and $^{206}Pb/^{204}Pb$ in the range 18.06–18.67, and high $^{143}Nd/^{144}Nd$ ratios (0.51312–0.51322), similar to basalts of the East Pacific Rise (Bach *et al*. 1994). However, some Chile Ridge basalts (Klein & Karsten 1995; Fig. 1e) have high Ba/La (up to 22; Fig. 8), $^{87}Sr/^{86}Sr$ (up to 0.7035; Fig. 10) and $^{206}Pb/$

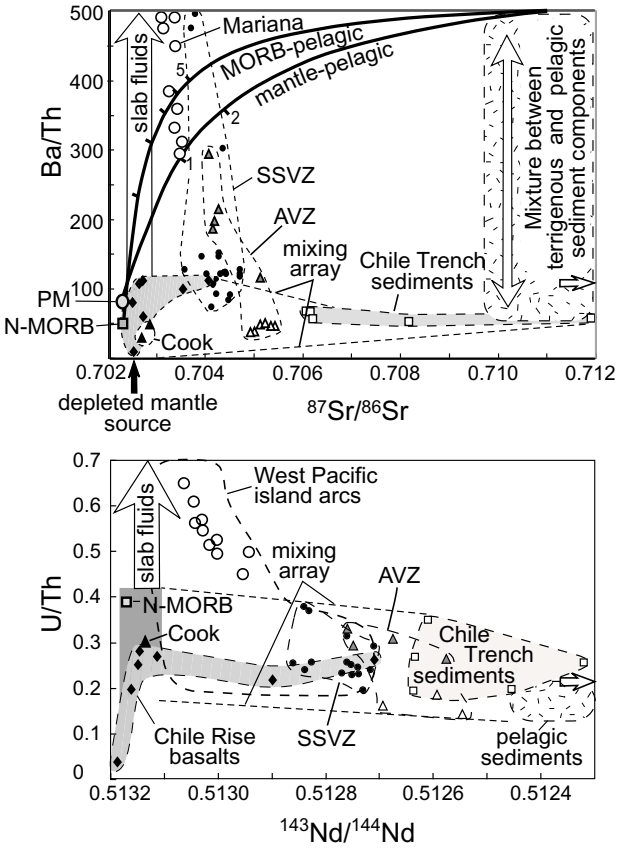

Fig. 10. (**a**) Ba/Th v. $^{87}Sr/^{86}Sr$ and (**b**) U/Th v. $^{143}Nd/^{144}Nd$, with plots for N-MORB and Primitive Mantle (PM; Sun & McDonough 1989), Chile Rise basalts (; Klein & Karsten 1995), adakites of the Andean Austral Volcanic Zone (AVZ; Stern & Kilian 1996; ▲, Cook Island; △, N-AVZ; grey triangles, C-AVZ; for locations see Fig. 1a), basalts of the Andean southernmost Southern Volcanic Zone (SSVZ, ●; Lopez-Escobar *et al*. 1993; Kilian 1997), Global Subducting Sediment (GLOSS, open arrow; Plank & Langmuir 1998), and investigated Chile Trench sediments and pelagic sediments from the Antarctic Plate. ○, basalts of Mariana arc. Mixing arrays between MORB and Chile Trench sediments and arrows for MORB-derived fluids are indicated. Also shown are mixing lines between a primitive mantle and pelagic sediments and between MORB and pelagic sediment. Numbers on the lines indicate weight per cent of mixture.

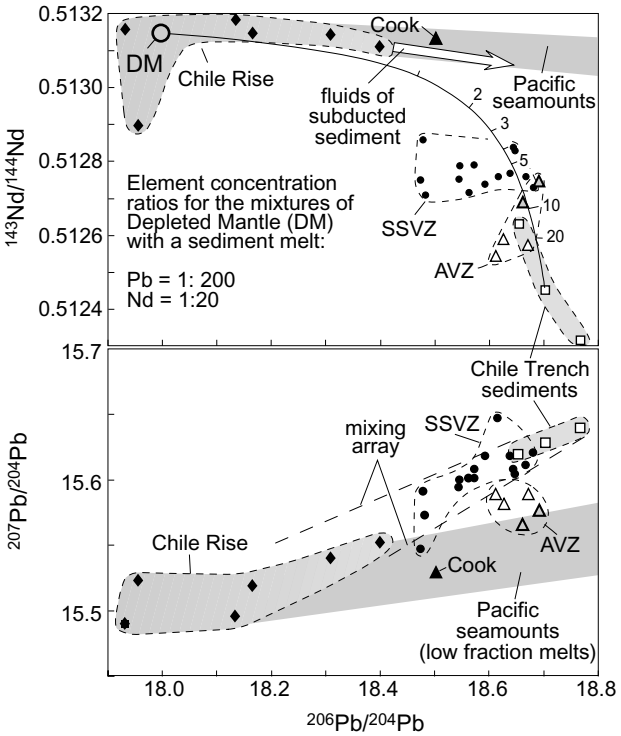

Fig. 11. $^{143}Nd/^{144}Nd$ and $^{207}Pb/^{204}Pb$ ratios, each plotted v. $^{206}Pb/^{204}Pb$ ratios for trench sediments of ODP Leg 141, Chile Rise basalts, basalts of the Andean southernmost Southern Volcanic Zone (SSVZ) and adakites of the Andean Austral Volcanic Zone (AVZ). (For references for the data and further explanation, see Fig. 10 caption.) Mixing of a subducted sediment-derived melt (with tick marks for vol.% sediment melt) within a depleted mantle (DM) is shown.

^{204}Pb ratios (up to 18.40; Fig. 11) as well as low Ce/Pb (14–25) and $^{143}Nd/^{144}Nd$ ratios (0.5127; Fig. 10), indicating contamination with subducted terrigenous sediments (or melts derived therefrom), similar in composition to the Chile Trench sediments. Some Chile Ridge basalts also have high Ba/Th ratios (up to 120; Klein & Karsten 1995), suggesting a previous contamination by slab fluids and/or by Ba-rich pelagic sediments (Figs 8 and 10a). Chemical characteristics of the Chile Ridge basalts suggest that the asthenospheric mantle below the investigated area is chemically and isotopically depleted, but contains some enriched components similar to the investigated sediments, which may give an important geochemical fingerprint in low-fraction melts. Mantle xenoliths from the mantle wedge below the Southern Andes also indicate a predominantly depleted mantle wedge that occasionally contains adakitic glass veins and enriched components derived from subducted MORB and/or sediments (Kilian & Stern 2002).

Sediment recycling in the Andean southernmost Southern Volcanic Zone (SSVZ; 41–47°S)

North of the plate triple junction, the Nazca Plate is subducted relatively fast (8–9 cm a^{-1}) below the Andes (Fig. 1). This leads to the formation of basaltic to dacitic calc-alkaline rock suites of the SSVZ (Figs 1a and 2; Lopez-Escobar *et al*. 1993; Kilian 1997). Although the subducted Nazca Plate is relatively young (2–18 Ma), there is no adakite formation, suggesting melting of subducted MORB (Kilian 1997). However, temperatures may be high enough to form melts in subducted sediments (Peacock *et al*. 1994). Below we discuss possible source contaminations for SSVZ basalts with high Mg-number (>50), for which crustal contamination is limited and chemical as well as isotopic tracers of basaltic to dacitic fractionation trends do not indicate significant crustal contamination (Lopez-Escobar *et al*. 1993; Kilian 1997). The relatively low Nb and Ta contents (Fig. 4) of the SSVZ basalts suggest that they were formed at relatively high degrees of partial melting from a relatively depleted mantle wedge (Pearce *et al*. 1994).

Basalts of the SSVZ have moderately low U/Th ratios (0.2–0.4; Fig. 10b), similar to MORB and in the same range as the ODP Leg 141 sediments and investigated pelagic sediments. They do not show the high U/Th ratios (up to 0.7) reported for some basalts of the Western Pacific arcs, specifically the Mariana arc, for which a significant contribution by slab fluids was suggested (Elliott *et al*. 1997; Hawkesworth *et al*. 1997). In the plot of U/Th v. $^{143}Nd/^{144}Nd$ ratios (Fig. 10b), the SSVZ basalts fit well into a mixing array between MORB (including Chile Rise basalts: Klein & Karsten 1995), representing the depleted mantle wedge before slab contamination, and ODP Leg 141 sediments as well as the investigated pelagic sediments from the SE Pacific.

The Ba/Th ratios of the SSVZ basalts are most variable (Ba/Th = 75–500; Fig. 10a) and partly significantly higher than N-MORB (Ba/Th = 10–110), Chile Trench sediments (Ba/Th = 45–73), Palaeozoic S-type crust (average Ba/Th = 57), I-type plutonic crust (average Ba/Th = 68) as well as an average lower crust (Ba/Th = 136; Taylor & McLennan 1985). These values also exclude significant upper-crustal contamination for the high-Ba SSVZ basalts of Hudson volcano (46°S; Figs 2 and 10a). Only the contamination by Ba-rich MORB-derived fluids, as suggested for basalts from the Mariana arc and other Western Pacific arcs (Elliott *et al*. 1997; Hawkesworth *et al*. 1997), and/or contamination by Ba-rich pelagic sediments, as observed in the Western Pacific (Hole *et al*. 1984) and on the Antarctic Plate (Table 2), can explain the high Ba/Th ratios of these SSVZ basalts. As the U/Th ratios of the SSVZ basalts do not indicate contamination by slab fluids, we suggest that the mantle source of the SSVZ basalts was contaminated by, in addition to subducted Chile Trench sediments, variable amounts of Ba-rich pelagic sediments. In the plot of Ba/Th v. $^{87}Sr/^{86}Sr$ ratios (Fig. 10a) some SSVZ basalts plot into the mixing array between a MORB-like mantle source and Chile Trench sediments. Other SSVZ basalts lie on a mixing line between such a mantle source and 1–3 wt.% of a Ba-rich pelagic sediments. This suggests a three-component mixture of a depleted mantle with terrigeneous sediments and generally little, but sometimes much, high Ba/Th pelagic sediments.

The plots of $^{206}Pb/^{204}Pb$ v. $^{207}Pb/^{204}Pb$ and v. $^{143}Nd/^{144}Nd$ (Fig. 11) also indicate that a previously depleted mantle source of the SSVZ basalts was contaminated with 3–5 wt.% of a terrigenous sediment-melt, but not with sediment-derived fluids. The latter would not produce the observed decrease in the $^{143}Nd/^{144}Nd$ values (white arrow in the upper part of Fig. 11).

Sediment recycling in the Andean Austral Volcanic Zone

South of the plate triple junction, the Antarctic Plate has an age of 12–20 Ma, and is slowly subducted (2–3 cm a^{-1}) below the Andes, probably resulting in a still 'hotter' subduction zone compared with the SSVZ (Fig. 1; Peacock *et al*. 1994). Together, this geodynamic feature and geochemical characteristics indicate that partial melts of the subducted eclogitic MORB, mixed with variable amounts of melts from subducted sediment, formed the

volcanic rocks of the Andean Austral Volcanic Zone (adakites with very high Sr/Y, Ta/Yb, La/Yb, Th/Yb ratios and Th excess; Stern & Kilian 1996; Sigmarsson *et al*. 1998; Kilian & Stern 2002). The high U/Nb and Th/Ta(Nb) ratios of the Andean Austral Volcanic Zone volcanic rocks also require melts from subducted MORB and sediments in equilibrium with a Ti phase, such as rutile.

Because of different chemical characteristics, we discuss the origin and sediment contribution for specific sections of the Andean Austral Volcanic Zone separately (Figs 1 and 2): the northern Andean Austral Volcanic Zone volcanoes Lautaro, Viedma and Aguilera (N-AVZ: 48–49°S), the central Andean Austral Volcanic Zone volcanoes Reclus and Burney (C-AVZ: 50–52°S) and the southernmost Andean Austral Volcanic Zone volcano Cook (55°S).

N-MORB-like Ba/La, Ba/Th and U/Th (e.g. Lundstrom *et al*. 1994), as well as the Sr, Nd and Pb isotopic ratios (Figs 10 and 11), and the very high Sr/Y and La/Yb ratios constrain an eclogitic MORB source for Cook volcanic rocks of the Andean Austral Volcanic Zone (Stern & Kilian 1996), excluding any contribution by Chile Trench or pelagic sediments.

Excess Th, high Sr/Y, and low Y and Yb concentrations of C-AVZ volcanic rocks (Fig. 1) and N-AVZ volcanic rocks indicate an origin from slab melts (Stern & Kilian 1996; Sigmarsson *et al*. 1998). In the U/Th v. $^{143}Nd/^{144}Nd$ plot (Fig. 10a) the N-AVZ and C-AVZ volcanic rocks plot into a mixing array between subducted MORB and terrigenous end-members, the latter being either Chile Trench sediments or investigated pelagic sediments of the Antarctic Plate. However, this diagram is not able to exclude some contribution by the continental crust.

In the Ba/Th v. $^{87}Sr/^{86}Sr$ plot (Fig. 10b) only the volcanic rocks of the N-AVZ plot into the mixing array between MORB and the Chile Trench sediments, or melts from both components. Volcanic rocks of the C-AVZ, related to the subduction of an older oceanic crust (*c*. 20 Ma), have relatively high Ba/Th ratios (110–300), suggesting contribution by Ba-rich pelagic sediments and/or slab-derived fluids (Elliott *et al*. 1997; Hawkesworth *et al*. 1997). Arguments against the latter come from the low U/Th ratios of volcanic rocks from the C-AVZ ($U/Th = 0.25$–0.35) and also from their very low Y (9–11 ppm) and Yb contents (Stern & Kilian 1996), which limit the contribution of basaltic melts from a fluid-metasomatized mantle, because such basalts commonly have high contents of Y (20–30 ppm; Hawkesworth *et al*. 1991; Kilian 1997).

Isotopic models with $^{87}Sr/^{86}Sr$, $^{143}Nd/^{144}Nd$, O and Pb isotopic characteristics of volcanic rocks from the C-AVZ suggest a mixture of 80–90 vol.% MORB melt with 10–20 vol.% sediment melt and only a small contribution by the upper continental crust (Stern & Kilian 1996). Mass balance calculations with the new Pb isotopic data of the Chile Trench sediments are consistent with this estimate. In the $^{206}Pb/^{204}Pb$ v. $^{207}Pb/^{204}Pb$ plot (Fig. 11), the volcanic rocks of the Andean Austral Volcanic Zone are placed on a mixing line between melts of a more radiogenic $^{206}Pb/^{204}Pb$ Pacific MORB and Chile Trench sediments (10–20 wt.%).

Conclusions

The chemical and isotopic compositions of Pliocene to Pleistocene Chile Trench sediments reflect variable contribution of chemically unaltered major rock lithologies of the Southern Andes without significant contribution by biogenic and/or chemical sediments. This indicates an almost closed system with high denudation, transport and deposition rates along the Southern Andes continental margin since 2.5 Ma. In contrast, pelagic sediments cored farther from the continent (>1000 km) represent significantly lower sedimentation rates. These sediments contain a smaller terrigeneous component (>80 vol.%), variable amounts of siliceous microfossils (2–12 vol.%) and manganese micronodules (1–3 vol.%). They differ chemically from the trench sediments by their significantly higher Ba/Th ratios (150–500) and negative Ce anomalies. Some Chile Ridge basalts as well as some adakites from the Andean Austral Volcanic Zone and a few basalts from the southernmost Andean Southern Volcanic Zone have high Ba/Th ratios and no slab fluid signature (low U/Th), suggesting subduction recycling of pelagic sediments. Crustal-related Sr, Nd and Pb isotopic signatures of all primitive basaltic and adakitic volcanic rocks of the Southern Andes together with a missing slab fluid signature (low U/Th and Ba/Th ratios) suggest that partial melts of subducted sediments, similar to those cored during ODP Leg 141, have contaminated the mantle wedge below the Southern Andes.

E. Hegner was very helpful in carrying out isotope analyses at the Institut für Mineralogie, Petrologie und Geochemie, Tübingen, Germany. We thank H. Miller (Munich) for providing rock samples from Chonos Archipelago, and R. J. Pankhurst for sending us unpublished data for a review of crustal compositions. H. J. Walter is thanked for providing sediment samples from an Antaratic Plate. R. Ellam, C. J. Hawkesworth, M. S. Kay, T. Ludwig, D. Peate and J. Tipper are thanked for suggesting improvements to the manuscript. A. Saunders and M. Fowler gave further constructive comments. We are grateful to the Ocean Drilling Program for providing the core samples used in this study. J.H.B. thanks all ODP Leg 141 scientists and technical staff for their enduring support at sea. The German Research Foundation (DFG) has supported R.K. (Grant Ki 456/1-4) and J.H.B. (Grant Be 1041/7).

References

Ayers, J.C., Dittmer, S.K. & Layne, G.D. 1997. Partitioning of elements between peridotite and H_2O at 2.0–3.0 GPa and 900–1100 °C, and application to models of subduction processes. *Earth and Planetary Science Letters*, **150**, 381–398.

Bach, W., Hegner, E., Erzinger, J. & Satir, M. 1994. Chemical and isotopic variations along the superfast spreading East Pacific Rise from 6 to 30°S. *Contributions to Mineralogy and Petrology*, **116**, 365–380.

Behrmann, J.H. & Kopf, A. 2001. Balance of tectonically accreted and subducted sediment at the Chile Triple Junction. *International Journal of Earth Science*, **90**, 753–768.

Behrmann, J.H., Lewis, S.D., Cande, S. & ODP Leg 141 Scientific Party 1994. Tectonics and geology of spreading ridge subduction at the Chile Triple Junction; a synthesis of results from Leg 141 of the Ocean Drilling Program. *Geologische Rundschau*, **83**, 832–852.

Behrmann, J.H., Lewis, S.D., *et al.* (eds) 1992. *Chile Triple Junction. Proceedings of the Ocean Drilling Program, Scientific Results, Initial Reports, 141*. Ocean Drilling Program, College Station, TX.

Brenan, J.M., Shaw, H.F., Phinney, D.L. & Ryerson, F.J. 1994. Rutile–aqueous fluid partitioning of Nb, Ta, Hf, Zr, U and Th: implications for high field strength element depletions in island-arc basalts. *Earth and Planetary Science Letters*, **128**, 327–339.

Brenan, J.M., Shaw, H.F., Ryerson, F.J. & Phinney, D.L. 1995. Mineral–aqueous fluid partitioning of trace elements at 900 °C and 2 GPa: constraints on the trace element chemistry of mantle and deep crustal fluids. *Geochimica et Cosmochimica Acta*, **59**, 3331–3350.

Brown, K.M. & Bangs, N. *et al.* 1995. A summary of ODP Leg 141 hydrogeological, geochemical, and thermal results. *In:* Lewis, S.D., Behrmann, J.H., Musgrave, R.J. & Cande, S.C. (eds) *Proceedings of the Ocean Drilling Program, Scientific Results, 141*. Ocean Drilling Program, College Station, TX, 363–371.

Cande, S.C. & Kent, D.V. 1992. A new geomagnetic polarity time scale for the Late Cretaceous and Cenozoic. *Journal of Geophysical Research*, **97**, 13917–13951.

Cande, S.C. & Leslie, R.B. 1986. Late Cenozoic tectonics of the southern Chile trench. *Journal of Geophysical Research*, **91**, 471–496.

Clapperton, C.M. 1990. Quaternary glaciations in the southern hemisphere: an overview of the Southern Andes. *Quaternary Science Reviews*, **9**, 299–304.

Diemer, J.A. & Forsythe, R. 1995. Grain size variations within slope facies recovered from the Chile Margin Triple Junction. *In:* Lewis, S.D., Behrmann, J.H., Musgrave, R.J. & Cande, S.C. (eds) *Proceedings of the Ocean Drilling Program, Scientific Results, 141*. Ocean Drilling Program, College Station, TX, 79–93.

Dymond, J., Suess, E. & Lyle, M. 1992. Barium in deep-sea sediment: a geochemical proxy for paleoproductivity. *Paleoceanography*, **7**, 163–181.

Elderfield, H. & Greaves, M.J. 1981. Negative cerium anomalies in the rare earth element patterns of oceanic ferromanganese nodules. *Earth and Planetary Science Letters*, **55**, 163–170.

Elliott, T., Plank, T., Zindler, A., White, W. & Bourdon, B. 1997. Element transport from slab to volcanic front at the Mariana arc. *Journal of Geophysical Research*, **102**, 14991–15019.

Grégoire, D.C., Ansdell, K.M., Glotz, D.M. & Chakraborti, C.L. 1995. Trace element analysis of single zircons for rare-earth element, U and Th by electrothermal vaporisation–inductively coupled plasma mass spectrometry. *Chemical Geology*, **124**, 91–99.

Hawkesworth, C.J. & Ellam, R. 1989. Chemical fluxes and wedge replenishment rates along recent destructive plate margins. *Geology*, **17**, 46–49.

Hawkesworth, C.J., Hergt, J.M., McDermott, F. & Ellam, R.M. 1991. Destructive margin magmatism and the contributions from the mantle wedge and subducted crust. *Australian Journal of Earth Sciences*, **38**, 577–594.

Hawkesworth, C.J., Turner, S., Peate, D., McDermott, F. & van Calsteren, P. 1997. Elemental U and Th variations in island arc rocks: implications for U-series isotopes. *Chemical Geology*, **139**, 207–221.

Herron, E.M., Bruhn, R., Winslow, M. & Chuaqui, L. 1977. Post Miocene tectonics of the margin of southern Chile. *In:* Talwani, M. & Pitman, W.C. III (eds) *Island Arcs, Deep Sea Trenches and Back-arc Basins*. American Geophysical Union, Maurice Ewing Series, **1**, 273–283.

Herron, E.M., Cande, S.C. & Hall, B.R. 1981. An active spreading centre collides with a subduction zone: a geophysical investigation of the Chile margin triple junction. *In:* Kulm, L.V.D., Dymond, J., Dasch, E.J. & Hussong, D.M. (eds) *Nazca Plate: Crustal Formation and Andean Convergence*. Geological Society of America, Memoirs, **154**, 683–701.

Hole, M.J., Saunders, A.D., Marriner, G.F. & Tarney, J. 1984. Subduction of pelagic sediments: implications for the origin of Ce-anomalous basalts from Mariana Islands. *Journal of the Geological Society, London*, **141**, 453–472.

Jenner, G.A., Longerich, H.P., Jackson, S.E. & Fryer, B.J. 1990. ICP-MS—a powerful tool for high-precision trace-element analysis in earth sciences: evidence from analysis of selected U.S.G.S. reference samples. *Chemical Geology*, **83**, 133–148.

Karl, S.M., Wandless, G.A. & Karpoff, A.M. *et al.* 1992. Sedimentology and geochemical characteristics of ODP Leg 129 siliceous deposits. *In:* Larson, R. & Lancelot, Y. (eds) *Proceedings of the Ocean Drilling Program, Scientific Results, 129*. Ocean Drilling Program, College Station, TX, **TX**, 31–80.

Keppler, H. 1996. Constraints from partitioning experiments on the composition of subduction-zone fluids. *Nature*, **380**, 237–240.

Kilian, R. 1997. Magmatismus und Stoffkreislauf an aktiven Kontinentalränden, untersucht am Beispiel der südlichen Anden. *Zeitschrift der Deutschen Geologischen Gesellschaft*, **148**(1), 105–152.

Kilian, R. & Stern, C.R. 2002. Constraints on the interaction between slab melts and the mantle wedge from adakitic glass in peridotite xenoliths. *European Journal of Mineralogy*, **14**, 25–36.

Klein, E.M. & Karsten, J.L. 1995. Ocean-ridge basalts with convergent-margin geochemical affinities from the Chile Ridge. *Nature*, **374**, 52–57.

Kurnosov, V., Murdmaa, I., Chamov, N., Chudaev, O., Eroshchev-Shak, V. & Shterenberg, L. *et al.*1995. Mineralogy of sediments from the Chile Triple Junction. *In:* Lewis, S.D., Behrmann, J.H. & Musgrave, R.J. (eds) *Proceedings of the Ocean Drilling Program, Scientific Results, 141*. Ocean Drilling Program, College Station, TX, 95–104.

Lamy, F., Hebbeln, D., Röhl, U. & Wefer, G. 2001. Holocene rainfall variability in Southern Chile: a marine record of latitudinal shifts of Southern westerlies. *Earth and Planetary Science Letters*, **185**, 369–382.

LaTourrette, T.Z. & Burnett, D.S. 1992. Experimental determination of U and Th partitioning between clinopyroxene and natural and synthetic basaltic liquids. *Earth and Planetary Science Letters*, **110**, 227–244.

LaTourrette, T.Z., Kennedy, A.K. & Wasserburg, G.J. 1993. Thorium–uranium fractionation by garnet: evidence for a deep source and rapid rise of oceanic basalts. *Science*, **261**, 739–742.

Longerich, H.P., Jenner, G.A., Freyer, B.L. & Jackson, S.E. 1990. Inductively coupled plasma-mass spectrometric analysis of geological samples: a critical evaluation based on case studies. *Chemical Geology*, **83**, 105–118.

Lopez-Escobar, L., Kilian, R., Kempton, P. & Tagiri, M. 1993. Petrography and geochemistry of Quaternary rocks from the Southern Volcanic Zone of the Andes between 41°30′ and 46°00′S, Chile. *Revista Geologica de Chile*, **20**, 33–55.

Lundstrom, C.C., Shaw, H.F., Ryerson, F.J., Phinney, D.L., Gill, J.B. & Williams, Q. 1994. Compositional controls on the partitioning of U, Th, Ba, Sr and Zr between clinopyroxene and haplobasaltic melts: implications for uranium series disequilibria in basalts. *Earth and Planetary Science Letters*, **128**, 407–423.

McMurtry, G.M., Veeh, H.H. & Moser, C. 1981. Sediment accumulation rate patterns on the northwest Nazca plate. *In:* Editor, A. (ed.) *Book title*. Geological Society of America, Memoirs, **154**, 211–250.

Miller, H. 1979. Das Grundgebirge der Anden im Chonos-Archipel, Region Aysén, Chile. *Geologische Rundschau*, **68**, 428–456.

Miller, H. 1984. Orogenic development of the Argentine/Chilean Andes during the Paleozoic. *Journal of the Geological Society, London*, **141**, 885–892.

Niu, Y. & Hékinian, R. 1997. Basaltic liquids and harzburgitic residues in the Garrett transform: a case study at fast spreading ridges. *Earth and Planetary Science Letters*, **146**, 243–258.

Pankhurst, R.J. & Hervé, F. 1995. Granitoid age distribution and emplacement control in the North Patagonian batholith in Aysen (44°–47°S). *Congresso Geologico Chileno, Actas*, **II**, 1409–1413.

Pankhurst, R.J., Hervé, F., Rojas, L. & Cembrano, J. 1992. Magmatism and tectonics in continental Chiloé, Chile (42°–42 30°). *Tectonophysics*, **205**, 283–294.

Peacock, S.M., Rushmer, T. & Thompson, A.L. 1994. Partial melting of subducted oceanic crust. *Earth and Planetary Science Letters*, **121**, 227–244.

Pearce, J.A., Parkinson, I.J. & Peate, D.W. 1994. Geochemical evidence for magma generation above subduction zones. *Mineralogical Magazine*, **58A**, 701–702.

Peucker-Ehrenbrink, B., Hofmann, A.W. & Hart, S.R. 1994. Hydrothermal lead transfer from mantle to continental crust: the role of metalliferous sediments. *Contributions to Mineralogy and Petrology*, **125**, 129–142.

Plank, T. & Langmuir, C.H. 1993. Tracing trace elements from sediment input to volcanic output at subduction zones. *Nature*, **362**, 739–743.

Plank, T. & Langmuir, C.H. 1998. The geochemical composition of subducting sediment and its consequences for the crust and mantle. *Chemical Geology*, **145**, 325–394.

Schiano, P., Clocchiatti, R., Shimizu, N., Jochum, K.P. & Hofman, A.W. 1995. Hydrous, silica-rich melts in the sub-arc mantle and their relationship with erupted arc lavas. *Nature*, **377**, 595–600.

Sigmarsson, O., Martin, H. & Knowles, J. 1998. Melting of a subducting oceanic crust from U–Th disequilibria in Austral Andean lavas. *Nature*, **394**, 566–569.

Staudigel, H., Davies, G.R., Hart, S.R., Marchant, K.M. & Smith, B.M. 1995. Large scale isotopic Sr, Nd and O isotopic anatomy of altered oceanic crust: DSDP/ODP sites 417/418. *Earth and Planetary Science Letters*, **130**, 169–185.

Stern, C.R. 1991. Mid-Holocene tephra on Tierra del Fuego (54°S) derived from the Hudson Volcano (46°S): evidence for a large explosive eruption. *Revista Geologica de Chile*, **18**, 139–146.

Stern, C.R. & Kilian, R. 1996. The role of subducted slab, mantle wedge and continental crust in the generation of adakites from the Andean Austral Volcanic Zone. *Contributions to Mineralogy and Petrology*, **123**, 263–281.

Stoffers, P., Glasby, G.P. & Frenzel, G. 1984. Comparison of the characteristics of manganese micronodules from the equatorial and south-west Pacific. *Tschermaks Mineralogische und Petrographische Mitteilungen*, **33**, 1–23.

Strand, K. 1995. SEM microstructural analysis of a volcanogenic sediment component in a Trench-slope basin of the Chile margin. *In:* Lewis, S.D., Behrmann, J.H., Musgrave, R.J. & Cande, S.C. (eds) *Proceedings of the Ocean Drilling Program, Scientific Results, 141*. Ocean Drilling Program, College Station, TX, 169–177.

Sun, S.S. & McDonough, W.F. 1989. Chemical and isotopic systematics of oceanic basalts: implications for mantle composition and processes. *In:* Saunders, A.D. & Norry, M.J. (eds) *Magmatism in Ocean Basins*. Geological Society, London, Special Publications, **42**, 313–345.

Taylor, S.R. & McLennan, S.M. 1985. *The Continental Crust: its Composition and Evolution*. Blackwell Scientific, Oxford.

Taylor, B. & Natland, J. 1995. *Active Margins and Marginal Basins of the Western Pacific*. Geophysical Monograph, American Geophysical Union, **88**.

von Huene, R. & Scholl, D.W. 1991. Observations on convergent margins concerning sediment subduction, subduction erosion, and the growth of continental crust. *Reviews of Geophysics*, **29**, 279–316.

Weaver, S.G., Bruce, R., Nelson, E.P., Brueckner, H.K. & Lehuray, A.P. 1990. The Patagonian batholith at 48°S latitudeChile; geochemical and isotopic variations. *In:* Kay, S.M. & Rapela, C.W. (eds) *Plutonism from Antarctica to Alaska*. Geological Society of America, Special Papers, **241**, 33–50.

Received 29 October 2001; revised typescript accepted 8 July 2002.
Scientific editing by Mike Fowler